STARS

Electronic Theses and Dissertations, 2004-2019

2013

Biomechanical Factors Influencing Treatment Of Developmental Dysplasia Of The Hip (ddh) With The Pavlik Harness

Orlando Ardila

University of Central Florida

BIOMECHANICAL FACTORS INFLUENCING TREATMENT OF DEVELOPMENTAL
DYSPLASIA OF THE HIP (DDH) WITH THE PAVLIK HARNESS

by

ORLANDO J. ARDILA
B.S. Florida State University, 2008

A thesis submitted in partial fulfillment of the requirements
for the degree of Master of Science
in the Department of Mechanical and Aerospace Engineering
in the College of Engineering and Computer Science
at the University of Central Florida
Orlando, Florida

Spring Term
2013

Major Professor: Alain J. Kassab

ABSTRACT

Biomechanical factors influencing the reduction of dislocated hips with the Pavlik harness in patients of Developmental Dysplasia of the Hip (DDH) were studied using a simplified three-dimensional computer model simulating hip reduction dynamics in (1) subluxated, and (2) fully dislocated hip joints. The CT-scans of a 6 month-old female infant were used to measure the geometrical features of the hip joint including acetabular and femoral head diameter, acetabular depth, and geometry of the acetabular labrum, using the medical segmentation software Mimics. The lower extremity was modeled by three segments: thigh, leg, and foot. The mass and the location of the center of gravity of each segment were calculated using anthropometry, based on the total body mass of a 6-month old female infant at the 50th length-for-age percentile. A calibrated nonlinear stress-strain model was used to simulate muscle responses. The simplified 3D model consists of the pubis, ischium, acetabulum with labrum, and femoral head, neck, and shaft. It is capable of simulating dislocated as well as reduced hips in abduction and flexion.

Five hip adductor muscles were identified as key mediators of DDH prognosis, and the non-dimensional force contribution of each in the direction necessary to achieve concentric hip reductions was determined. Results point to the adductor muscles as mediators of subluxated hip reductions, as their mechanical action is a function of the degree of hip dislocation. For subluxated hips in abduction and flexion, the Pectineus, Adductor Brevis, Adductor Longus, and proximal Adductor Magnus muscles contribute positively to reduction, while the rest of the Adductor Magnus contributes negatively. In full dislocations all muscles contribute detrimentally to reduction, elucidating the need for traction to reduce Graf IV type dislocations. Reduction of

dysplastic hips was found to occur in two distinct phases: (a) release phase and (b) reduction phase.

To expand the range of DDH-related problems that can be studied, an improved three-dimensional anatomical computer model was generated by combining CT-scan and muscle positional data belonging to four human subjects. This model consists of the hip bone and femora of a 10-week old female infant. It was segmented to encompass the distinct cartilaginous regions of infant anatomy, as well as the different regions of cortical and cancellous bone; these properties were retrieved from the literature. This engineering computer model of an infant anatomy is being employed for (1) the development of a complete finite element and dynamics computer model for simulations of hip dysplasia reductions using novel treatment approaches, (2) the determination of a path of least resistance in reductions of hip dysplasia based on a minimum potential energy approach, (3) the study of the mechanics of hyperflexion of the hip as alternative treatment for late-presenting cases of hip dysplasia, and (4) a comprehensive investigation of the effects of femoral anteversion angle (AV) variations in reductions of hip dysplasia. This thesis thus reports on an interdisciplinary effort between orthopedic surgeons and mechanical engineers to apply engineering fundamentals to solve medical problems. The results of this research are clinically relevant in pediatric orthopaedics.

This work is dedicated to my parents Orlando Ardila and Patricia Bonilla, my sister Natalia P. Radler, and my grandmother Gilma M. Mahecha, whose unconditional love and support made possible my professional preparation. Their instruction throughout life instituted in me the desire to make a difference in my field of expertise.

This work is also dedicated to Juan D. Montero for his unparalleled motivation, to my advisor Dr. Alain J. Kassab for his exceptional support and broad influential teachings, and to those who stood near irrespective of the intensity and time demands of my academic and professional responsibilities.

This work is ultimately dedicated to all the children that will benefit from the breakthroughs that we made in the treatment of Developmental Hip Dysplasia, and from the advances that we will continue to make employing the foundations provided by this work.

ACKNOWLEDGMENTS

TABLE OF CONTENTS

LIST OF FIGURES

LIST OF TABLES

CHAPTER ONE: INTRODUCTION

Hip dysplasia refers to an abnormal hip condition where misalignment, instability of the hip joint, or hip joint insufficiency without misalignment occurs. This condition affects 2-3 out of 1000 full term babies [1], and the Pavlik harness has become the standard of treatment for this disorder worldwide since its time of invention in the 1950's [2]. Original studies on the effectiveness of this harness were carried out on 1,912 patients showing failure of treatment in 15% of the cases[2], and this data was confirmed by a later study conducted at the Children's Hospital and Health Center in San Diego [3]. Additionally birth statistics confirmed over 2.4 million births in the United States for the year 2006, and preliminary data for 2008 shows a nearly identical trend [4].

With this in mind it is safe to predict that over 10,000 babies will be born each year with this detrimental disorder, of which nearly 1,600 will fail treatment with the Pavlik harness with devastating consequences, making it urgent to device a method by which the number of failures of treatment with this brace becomes significantly reduced in an attempt to reduce the health consequences in infants, distress in families, and to canalize the demands on the health care system to meet more critical demands, while making a positive impact in the economy by reducing the number of cases of hip dysplasia that require advanced treatment.

To this end we propose to develop a finite element computer model of infant hips realized from Computer Tomography (CT) and Magnetic Resonance Imaging (MRI) scanning data, that will make possible the determination of the optimum, patient-specific Pavlik harness load components, necessary to successfully vector the femoral heads into their correct physiological position in the acetabula, while maintaining hip reduction during the length of the

1

treatment for hip dysplasia in neonates. This will allow physicians to quantify the interacting forces and torques in order to develop optimized, patient-specific treatment plans that are shorter in length, and that will significantly reduce the incidence of treatment failure by this method.

As background, this study will be possible by the close partnership of physicians at the International Hip Dysplasia Institute (IHDI) and Orlando Health, with engineers at the Computational Mechanics Laboratory (CML) at the University of Central Florida. The medical professionals will obtain the necessary medical data and provide it to the CML team, who will develop the computer model to carry out the study.

Dr. Charles T. Price, director of IHDI will mediate the project, and will provide the engineering team with the International Hip Dysplasia Classification: the IHDI-developed, unique classification of the severity of neonate hip dysplasia by which this study will guide when reference to dysplasia degrees becomes necessary.

Additionally, the CML team also envisioned a follow-up study with this research as base that will make possible the systematic determination of optimum Pavlik harness configurations by developing and using an infant test dummy.

<u>Literature Review</u>

Overview

Hip dysplasia refers to an abnormal hip condition where misalignment, instability of the hip joint, or hip joint insufficiency without misalignment occurs. This condition is serious given that as many as 76% of osteoarthritis cases are attributed to untreated hip dysplasia patients, and

patients usually require total hip replacement before the age of 50[5]. During the early stages of life, abnormal positioning of the hip, depending on the severity, may present with asymmetrical leg lengths, a limp observed upon the onset of walking of the child, and in severe cases, motor/functional disabilities.

Hip dysplasia often presents during fetal development, and is found during the infant's examination at birth, in which case it is termed Congenital Hip Dysplasia (CHD), or in cases where infants are born with normal hips and the condition develops after birth, the condition is often referred to as Developmental Hip Dysplasia (DHD). Care must be exercised when reviewing work on the subject as terms have been used interchangeably.

Due to the well understood process of child development, it is well known that ligaments in a baby are loose, and the edges of the hip socket are made of cartilage that is soft and flexible. These parts ossify during the first year of life, making it crucial to detect hip dislocations as early as possible, and to immediately take corrective action to achieve reduction of the dislocation in order to take advantage of the growth potential of children during this time.

The most common, and currently used method of assessing and diagnosing hip dysplasia is by means of physical examination by the physician at the time of birth, and by then confirming the assessment using ultrasound [2]. Ultrasound is commonly used for visualizing hip instabilities, and numerous authors have discussed the assessment of hip dysplasia using this method. Clarke et al. completed an in depth study of the assessment of hip dysplasia using ultra sound, and discusses how the features of dysplasia can be identified [6].

Following assessment and diagnosis with hip dysplasia, the hips are visualized in a roentgenogram to determine the type and severity of the dislocation. Crowe at al. devised a ranking for dysplastic hips that is commonly used. In this ranking method, the amount of

subluxation can be determined form an anteroposterior roentgenogram of the pelvis using three landmarks: the pelvis height, the head-neck junction in the dysplastic hip, and the inferior margin of each teardrop. Based on his ranking, in percent subluxation, Crowe I: <50% subluxation, Crowe II: 50-75%, Crowe III:75-100%, Crowe IV:>100% [7]. This ranking can be observed in Figure 1.

Figure 1 - Hip Dysplasia Roentgenograms [8]

After an infant has been diagnosed with hip dysplasia, either CHD, or DHD, a reduction is promptly sought, in most instances using the Pavlik Harness, which as shown in Figure 2, consists of shoulder straps (1,2), a chest strap, two back straps (7,8), leg straps (5,6), and stirrups. This harness is designed to maintain the hips of an infant in abduction and flexion simultaneously as this position has shown to direct the femurs to their proper locations in the hip.
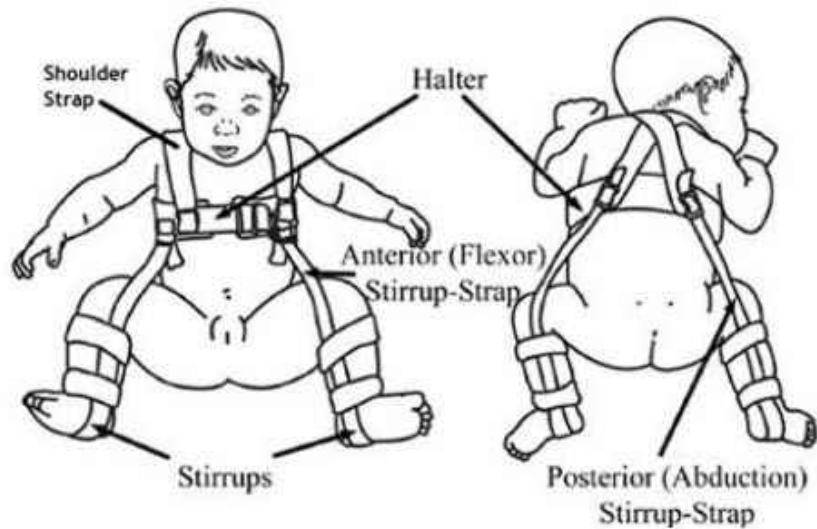
Figure 2 - The Pavlik Harness [2]

Considering the statistics of the disorder, nearly 1/20 full-term babies have some type of hip instability, and 2-3 out of 1000 babies will require treatment [1], for which the standard treatment worldwide has become the Pavlik harness [2; 9]. This harness is indicated for infants between one and nine months of age, with its maximum effectiveness achieved when the harness is worn shortly after birth; it is nevertheless contraindicated when there is muscle imbalance, major stiffness, or ligamentous laxity[2]; for the vast majority of children, however, the Pavlik harness is appropriate. This harness in certain circumstances fails to achieve reduction of the dislocated hips, and if unrecognized early, the failure brings tremendously adverse consequences for the child, the family, and the physician.

The major problems that have been reported to occur with the use of the Pavlik harness are failure to achieve concentric reduction, and avascular necrosis[2]; other problems found are delayed acetabular development, failure to stretch the hip adductors, femoral nerve palsy, and inferior (obturator) dislocation [3; 10]. Mubarak et al, along with other authors discuss that in the

5

cases studied the physicians never indicated whether the hip dislocation was reducible during the initial examination [3].

Because all of the above mentioned complications, failure of the Pavlik harness may lead to surgical procedures where risks are involved, osteoarthritis, avascular necrosis, and other serious disabilities, therefore it is clear that a method to assert reduction of hip dislocation using the Pavlik Harness is crucial, while drifting away from the believe that it can only achieve reduction due its passive mechanical factors coming into play during muscle relaxation in deep-sleep[11], and while finding an active way to achieve reduction as opposed to relying on clinical and ultrasound predictors [12], as it has been the common practice until now .

With the Pavlik harness in mind, and the imperative necessity to actively vector the femoral heads into the acetabula to achieve one-time reductions of the hips of the patients in necessity, and to actively monitor position during treatment with the Pavlik harness, a review of the pertinent literature was done with emphasis in the future analysis of the Pavlik-Harness-body interaction by means of the finite element method, and with the sole goal to achieve the worldwide desired solution to this common problem.

The Mechanical Properties of Infant Bone Tissue

To initialize a discussion on modeling the kinematics of the hip in response to variations in the application of forces by the Pavlik Harness, it is first necessary to discuss mechanical properties of bone in infants; One such study conducted using fresh autopsy femurs of infants reports the ultimate tensile stress, ultimate tensile strain, and tangent modulus of elasticity in tension as $10N/mm^2$, 1.850%, and $1012.9kg/mm^2$ respectively[13].

The Biomechanics of the Hip

Several investigations have been carried out to characterize the biomechanics of the hip and to quantify the differences between normal hips and those of dysplastic hips by quantifying the common forces, and their location.

Early studies of the hip identified and quantified its biomechanics using several different techniques. Maquet studied the biomechanics of hip dysplasia, and identified the force balance maintained in the hip during walking. In his study he identified three main forces, K, M, and R as shown in Figure 3. Force K is the force imposed on the hip by the body due to its weight, accelerations, decelerations and inertial forces, and acts with a lever arm h' from its line of action to the center of the femoral head. The moment of this force and perpendicular distance is balanced by the abductor muscle force, M, and its moment arm, which acts from its attachment at the greater trochanter to the center of the femoral head. The reaction force transmitted through the femur to the hip bone was denoted as R, and can go up more than 4 times the body weight during normal walking [14].

— Forces exerted on a loaded hip. S_5 centre of gravity of the mass of the body supported by the hip ; K force exerted by the mass of the body supported by the joint ; h' lever arm of K ; M force exerted by the abductor muscles ; h lever arm of M ; R force transmitted across the joint (= resultant of forces K and M).
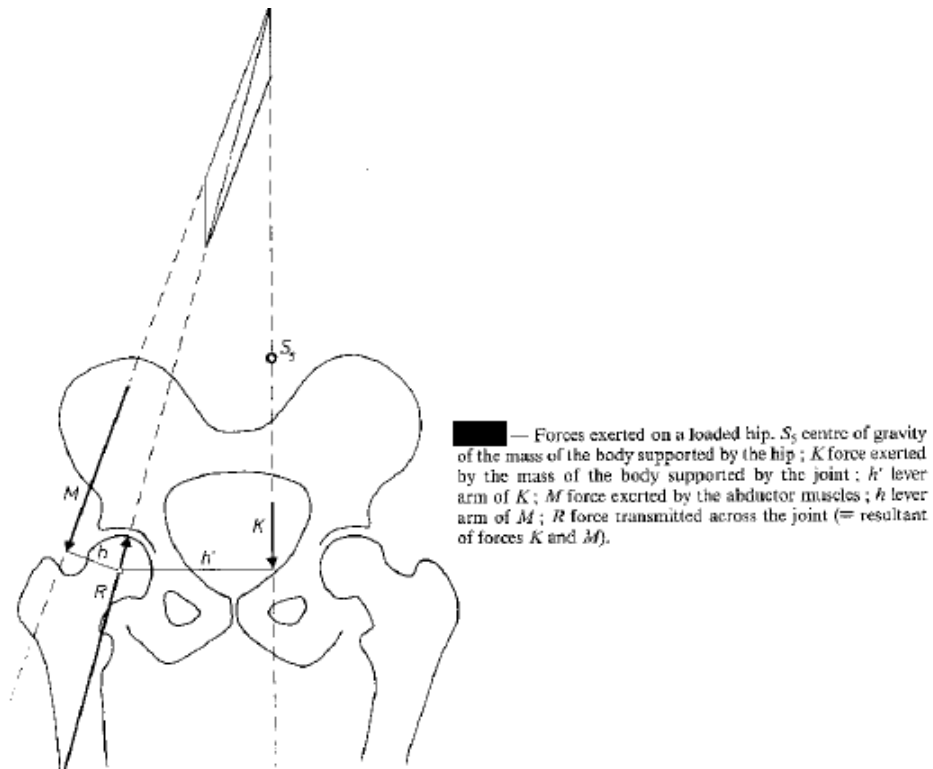
Figure 3 - Biomechanics of the Hip [14]

Maquet also identified the shift in forces common in dysplastic hips, Figure 4: a shortening of the lever arm h such as in coxa valga results in a larger and more vertical force M, necessary to counterbalance force K, displacing the resultant R towards the end of the socket, resulting in a decreased weight bearing, thus increasing the articular compressive stresses. Furthermore, a lengthening of the lever arm h, such as the case in coxa vara, allows for a decrease of the force M, necessary to counterbalance force K; the lengthening of this lever arm opens the angle between forces K and M, and the resultant R is displaced medially in the acetabulum causing an increase of articular compressive stresses in that region. Additionally, if the dysplasia is due to insufficiency of the acetabulum, the stress is unevenly distributed around the resultant R and greater in magnitude near the superior edge of the acetabulum, increasing

8

joint pressure there as depicted in Figure 4. In all deviations from normal hip configuration the distribution of stresses is uneven around the line of action of the resultant R, decreasing the weight bearing surface of the joint, causing premature wear of the cartilage resulting in subchondral sclerosis, and if untreated, the onset of osteoarthritis [14].
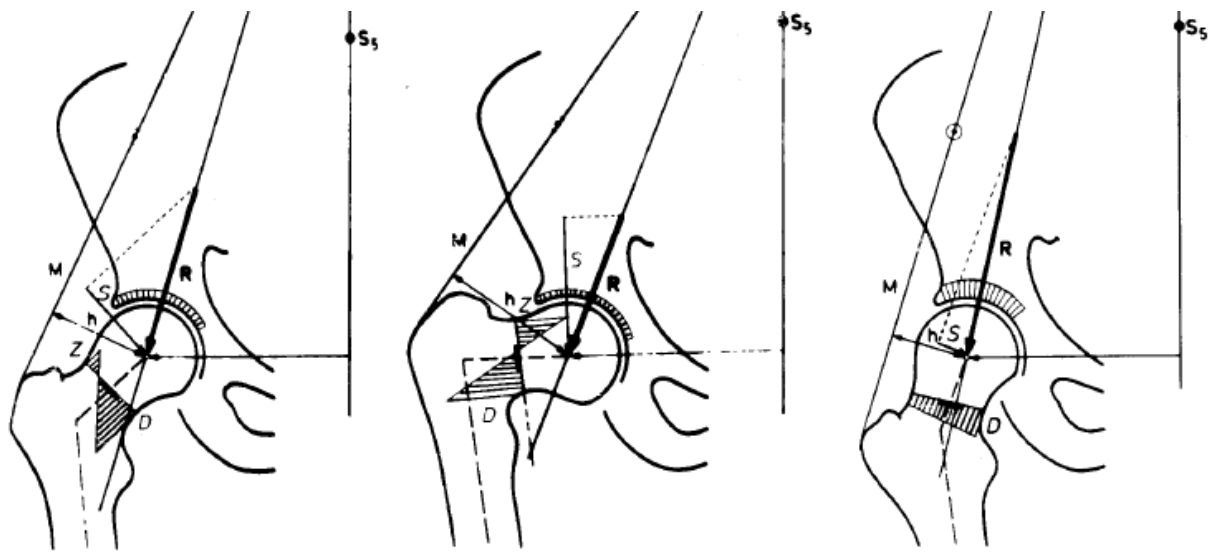
■ — Same signs as in Fig. 1. S shear ; D compression ; Z tension. The core of the neck is indicated by a black line. *a* normal hip ; *b* coxa vara ; *c* coxa valga (Maquet, 1985 ; after Pauwels, 1973).

Figure 4 - Dysplastic Hip Configurations [14]
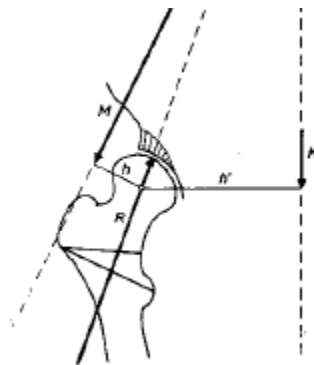
Figure 5 - Dysplasia due to acetabular insufficiency [14]

Additionally, the work of Bombelli et al. discusses the mechanics of the hip, and is in agreement with the work of Maquet. He also resolved the forces in the hip into components, and reported the vector consequences of varying degrees of acetabular dysplasia [15].

During an investigation of torsion in the femur, Fabry et al. reported that children with congenital hip dislocation, on average, had a greater angle of anteversion than children with normal hips. His observations apply to both hips in bilateral, as well as unilateral dislocation patients; Figure 6, Figure 7, along with Table 1 summarize their observations [16]:
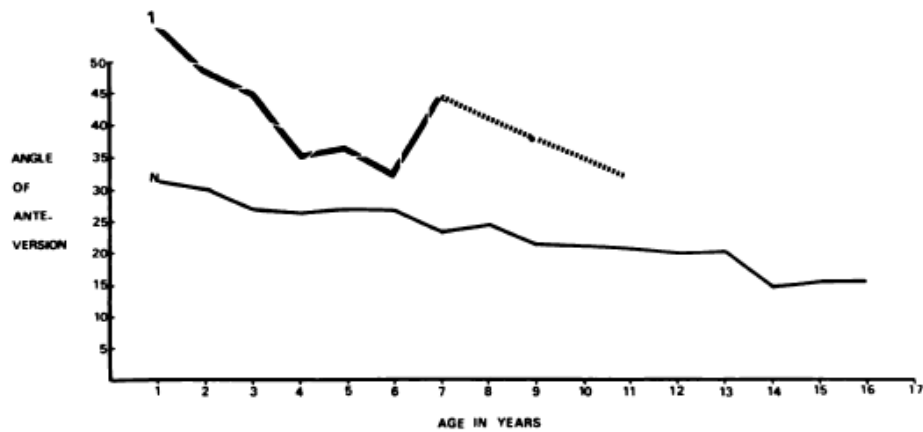
Femoral anteversion in 151 studies of ninety-three patients with congenital hip dislocation (1), plotted against the normal curve (N). The curve was not extended beyond the age of eleven years, because of the small number of hips examined in children older than eleven.

Figure 6 - Comparison Femoral Anteversion in Normal (N) and CHD (1) [16]

10
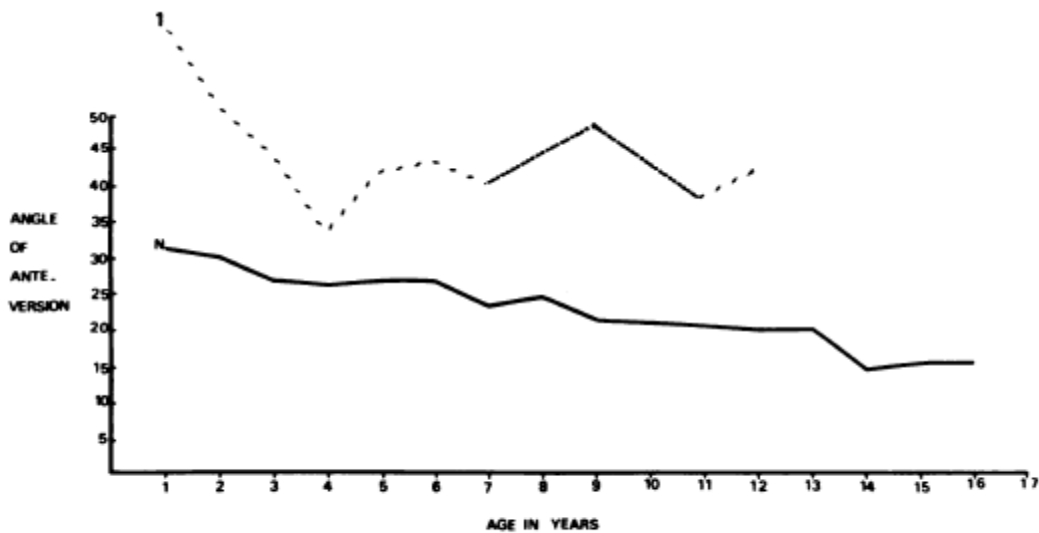
Anteversion in 120 studies of so-called normal hips in seventy-nine patients with unilateral hip dislocation (1) compared with normal anteversion (N).

Figure 7 - Comparison of unaffected hips (1) with normal hips in unilateral hip dislocation

Table 1 - Average anteversion (degree) in normal hips, and unaffected hips in unilateral hip dislocation

SIX YEARS AND TWO MONTHS' AVERAGE FOLLOW-UP OF FORTY-ONE UNAFFECTED HIPS IN PATIENTS WITH CONGENITAL DISLOCATION OF THE HIP

	Average Anteversion (Degrees)
Unaffected hips, first study	44.62
Unaffected hips, second study	41.59
Normal hips	24.14

Accurate measurement of the femoral torsion angle presented a challenge for orthopedists for a long time; this angle is that between the plane of the central axis of the femoral neck, and the plane of the transcondylar lower-end axis [17], as shown in Figure 8.

11
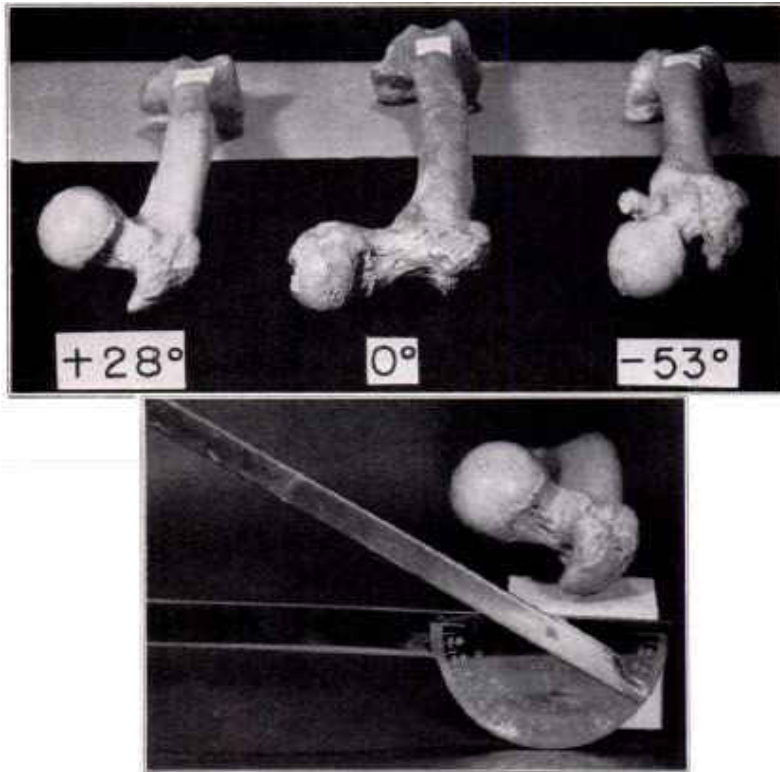
Figure 8 - Femoral torsion angle [17]

Dunlap et al., who also report abnormal femoral torsion angles in patients of CHD, devised a method where two roentgenograms of the patient are taken, one lateral, and one postero-anterior, and the torsion angle was then determined from the apparent torsion and apparent inclination as seen in the roentgenograms, with the use of a specially developed trigonometric formula [17]. They also discuss that difficult dysplasia cases correlate with moderate or greater degrees of torsion, and that torsion in the femur makes dysplastic hips less stable after reduction. Other research teams have also investigated different ways of measuring the torsional angle. Hernandez et al was able to measure femoral torsion angle using a CT scan, as shown in Figure 9 , and another research group achieved simple measurement of this angle using ultra sound [18].
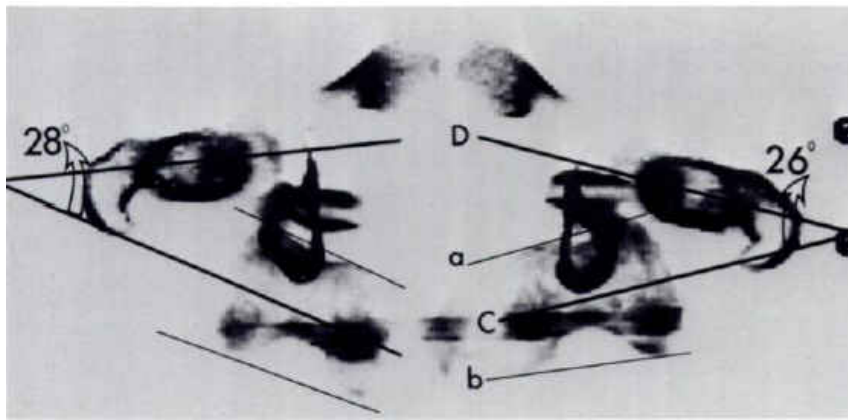
—Measuring the angles. Both sections of the femurs are superimposed with reverse polarity. Axis of femoral condyle (line C) is bisector of angle between tangents to anterior (line a) and posterior (line b) margins of femoral condyles. Line D is axis of femoral neck. Femoral torsion is angle between line C and line D (in this case, 28° on right, 26° on left).

Figure 9 - Torsion angle measured using CT scan [19]

Up to present there is no standard way to predict the outcome of treatment with the Pavlik harness, other than clinical and ultrasound observations and trends obtained from experience, some of which identify some characteristics of the condition of infants whose treatment in the Pavlik Harness often fails. There lacks in literature a standard method under which the forces and stability that the harness imposes on the femoral bones relative to the pelvic bones are measured, and the relative movement and position of these bones predicted based on the anatomical features of the patient, taking into consideration the resistance to movement imposed by ligaments, muscles, and the type of dislocation itself.

With a method to actively vector the femoral heads into their correct position, even a time period necessary for spontaneous reduction may be predicted and the total length of the treatment may therefore be accurately estimated based on the time of reduction and the biological changes that are known to occur in the hip bones in the early stages of child development, and in this way

reducing the risks associated with the trial-and-error based use that has been given to the Pavlik harness from its time of invention.

The Finite Element Method in Orthopedics

A number of researches have accomplished the mechanical quantification of musculoskeletal interactions successfully in different ways using a variety of approaches that provide solid insight on the different ways in which an orthopedic device such as the Pavlik harness, can be analyzed mechanically and the outcome of treatment reliably predicted by applying engineering fundamentals to the mechanical and biological interactions of the pelvic griddle with the femurs during treatment of Hip Dysplasia, whether congenital, or developmental.

Numerous researchers have attempted to use the advancement of technology in their favor; among them is the work of Michaeli et al.; in his study a computerized method for predicting joint contact pressures was evaluated for normal and dysplastic hips. This method uses images from a Computer Tomography (CT) scan and applies known hip joint reactions to the generated three dimensional surface of the hip joint. To achieve a prediction of surface pressures, the joint surface was discretized into squared elements, and the applied load was modeled as the resultant of many individual loads acting on the joint surface at each element. The group that conducted this study used cadaveric pelves along with plastic pelves models, and claim that the computer model could be used to predict pressure in the cadaveric pelves at prescribed locations, as well as magnitude and location of maximum pressure in the plastic models where the load vector, and degree of dysplasia were parametrically varied [5].

14

Additional work was contributed by Quesada, who conducted an investigation by means of the finite element method to find the proper modifications necessary in prostheses to increase their comfort. In this investigation a three-dimensional model of the prosthesis was discretized using quadrilateral and triangular shell elements with plane and bending stress behavior, as seen in Figure 10. At any point where the prosthesis and the stump soft tissue were in contact, the force exerted by the soft tissue on the socket was modeled by supporting the socket of the prosthesis at each node with springs with linear spring constants in each Cartesian direction, and the force on each socket node was then calculated as the sum of two forces: skin tensile, and soft tissue compressive forces. An approximation of the elastic coefficient of skin was also employed [20].
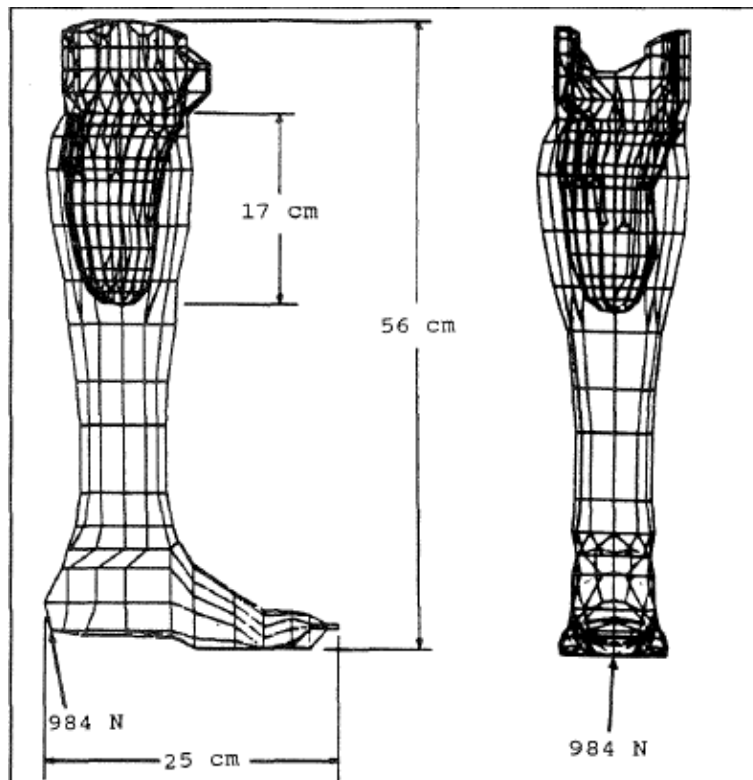
Figure 10 - Prosthesis discretized [20]

For the analysis of the orthopedic interactions one important requirement is the capability of accurately determining stresses in the interacting bones. Brown et al studied the distributions of mechanical stress in the proximal femur using the finite element stress analysis technique. With this technique, the structures of interest are discretized, or divided into regions, known as elements, bounded by nodes where information is either known, or approximated. This can be seen in Figure 11.
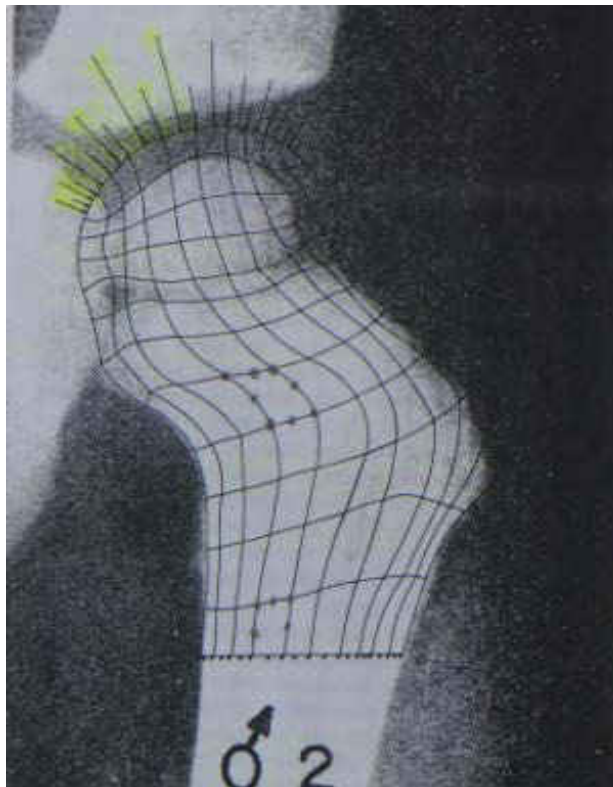
Figure 11 - Femur Discretization [21]

Using the finite element method approach irregular geometries with complicated distributions of material and complex loading patterns can be analyzed, and the value of physical quantities like stress, strain, or displacement can be approximated mathematically using known

conditions at adjacent nodes [21] . This technique has been used in the study of orthopedic interactions, and has a promising future in the analysis of the mechanics of the Pavlik harness interactions with the femur and hip bones in infants.
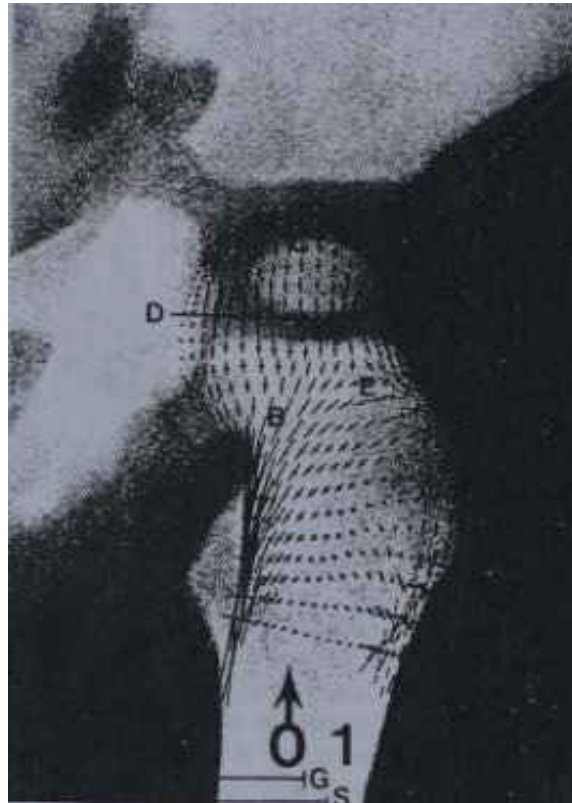
Figure 12 - Principal Stress Distribution [21]

Brown et al divided the proximal femur into 120 sub-regions of curvilinear shape, with eight nodes per element: one node on each corner and one node in the middle of each side, and was able to assemble experimentally measured tissue stiffness values into a global mathematical expression characterizing the overall behavior of the structure when subjected to different loads. In regions of significant material changes he created boundaries at the interface, and calculated

17

the resultant joint and muscle forces using principles of static equilibrium, modeling joint distributed contact forces as small discrete forces acting on each node of the interface.

In terms of forces, he evaluated the hip joint, and abductor muscle forces in terms of body weight and anatomical landmarks, where the lines of action of forces due to body weight, joint contact force, and abductor muscle were determined geometrically based on surgical experience, and used fresh autopsy samples subjected to compression tests to determine the elastic modulus values of the bones in question.
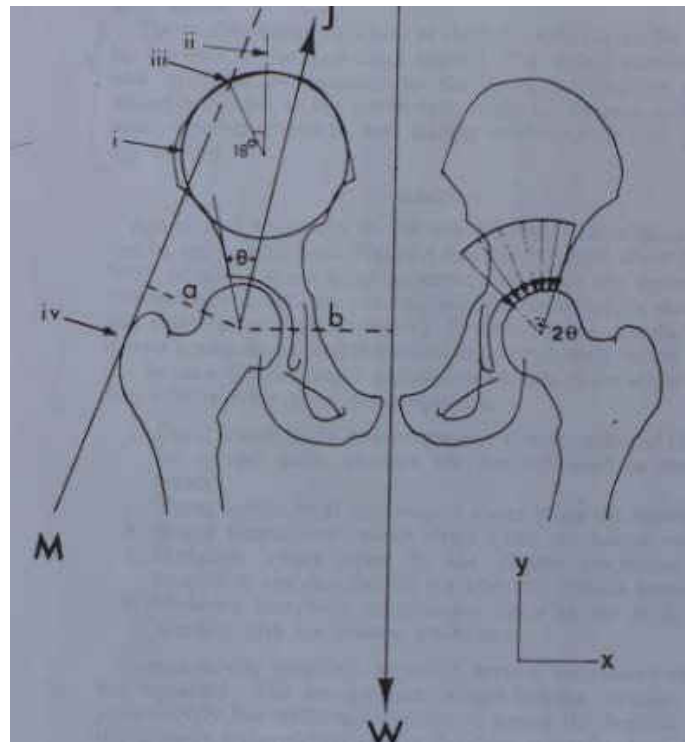
Figure 13 - Hip Forces [21]

Other studies have also attempted to take advantage of the advancement in technology; among the additional studies that have used the finite element method to study the mechanics of

18

the hip is that of Oonushi et al., who determined the deformations and displacements of the whole pelvis, including the pelvic ring, and the acetabulum, as well as the principal stresses, maximum shear stress, and Von Misses stress.

They obtained a three dimensional model of the pelvis using data from a CT scan as shown on Figure 14, and discretized it using solid elements for regions of cancellous bone, and membrane elements for regions of cortical bone as can be seen on Figure 15. Further discussion on their elements recommends the use of membrane elements for cortical bone, as shell elements connected to solid elements may yield unexplained discrepancies in displacement.

Solid elements consisting of tetrahedrons, pentahedrons, and hexahedrons, were used for discretization of the anatomy, and membrane elements were attached to the surface. Finally, 2251 elements, 930 nodal points, and 28 muscular elements were used.
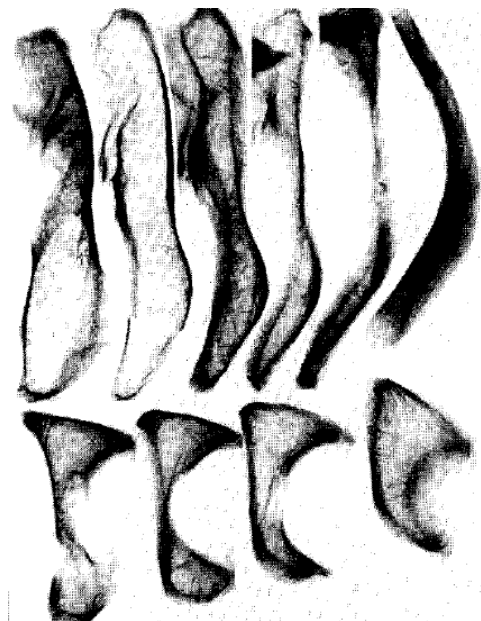
Figure 14 - CT Scan of the Pelvis [22]
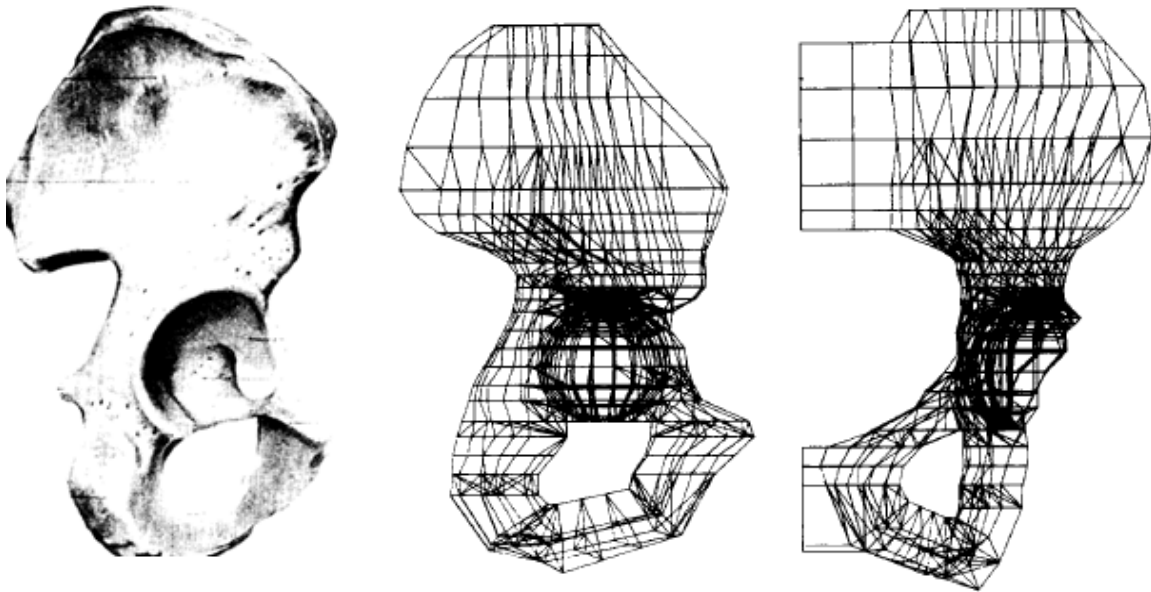
Figure 15 - Pelvis Discretization [22]

This group took advantage of the symmetry of the pelvis to simplify the work, and analyzed only the left side of the pelvis, applying boundary conditions at the line of symmetry to account for the part not analyzed, and assumed the acetabulum to be part of a spherical surface, constraining the femoral head and the acetabulum only in the normal direction in about 25 nodal points located in the weight bearing region of the joint as appreciated on Figure 16.
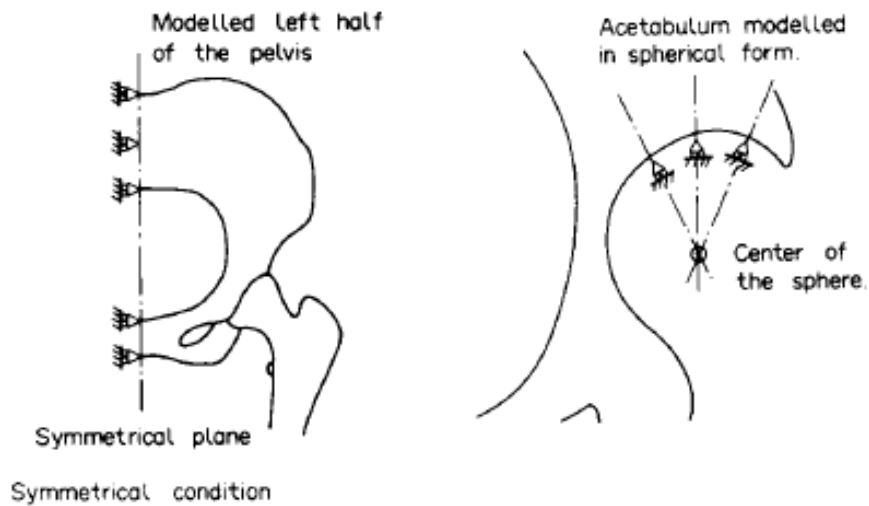
Figure 16 - Boundary Conditions [22]

In their model they differentiated between cancellous bone, cortical bone, subchondral bone, and cartilage, assigning a 1mm thickness layer of cortical bone covering cancellous bone, and the forces imposed by muscles were modeled as truss elements with stiffness only in the axial direction, and attachment only at two nodal points, one at each end, and each having degrees of freedom only in the u, v, and w coordinate directions[22]. See Figure 17.
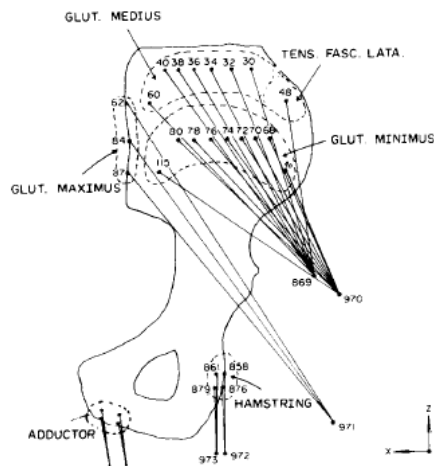
Figure 17 - Muscular Model [22]

21

As a final note on the use of the finite element method, Vaverka et al. conducted an in depth stress analysis in the physiological, as well as the dysplastic hip, as shown in Figure 18 and Figure 19 using this method. In this study images from a CT scan were again used to render 3 dimensional surfaces of the hip, which were later discretized into nodes and elements as previously described to create a finite element model in the software ANSYS 7. This group modeled the pelvic bone, femur, articular cartilages, and hip abductors; the later were modeled as highly stiff cables [23], as seen on Figure 20.

M. Vaverka et al. / Stress and strain analysis of the hip joint using FEM
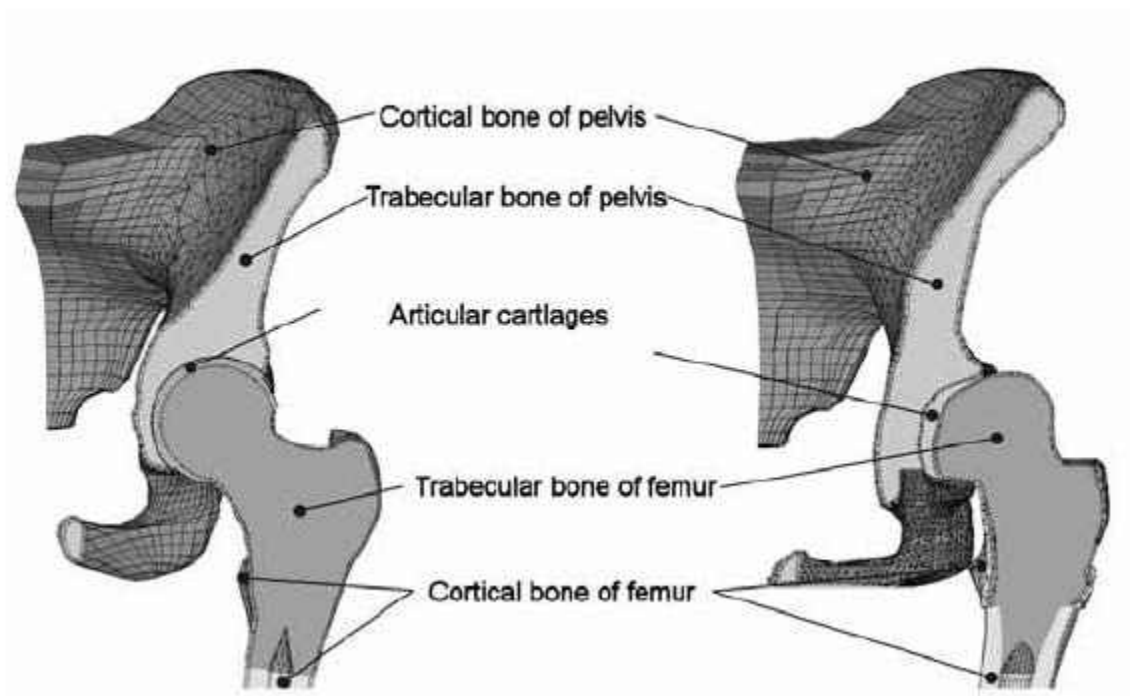
Figure 18 - Physiological (L) and Dysplastic (R) hip joints
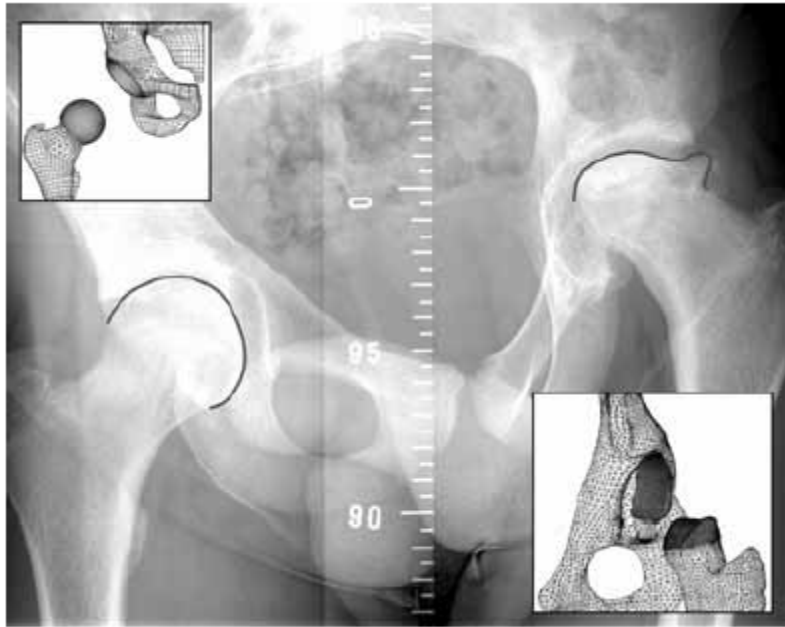
Figure 19 - Physiological (L) and Dysplastic (R) Hip Joints II
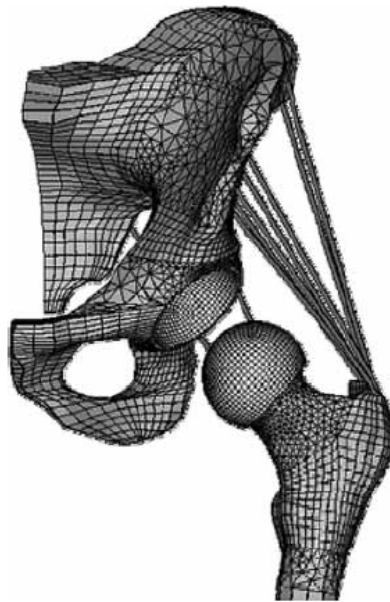
Figure 20 - FE Model of the Hip Joint

Finally material properties of individual tissues were modeled as homogeneous, isotropic with linear behavior, and described by Young's modulus, and Poisson's ratio, and the stresses and strains were calculated for both hips, as appreciated in Figure 21 and Figure 22. For this study, the highest stress in the dysplastic hip was nearly 20 times greater than that for the normal joint [23], which explains the premature degeneration of cartilage and bone tissue in dysplastic hips contributing to the high percentage of osteoarthritis cases previously described.
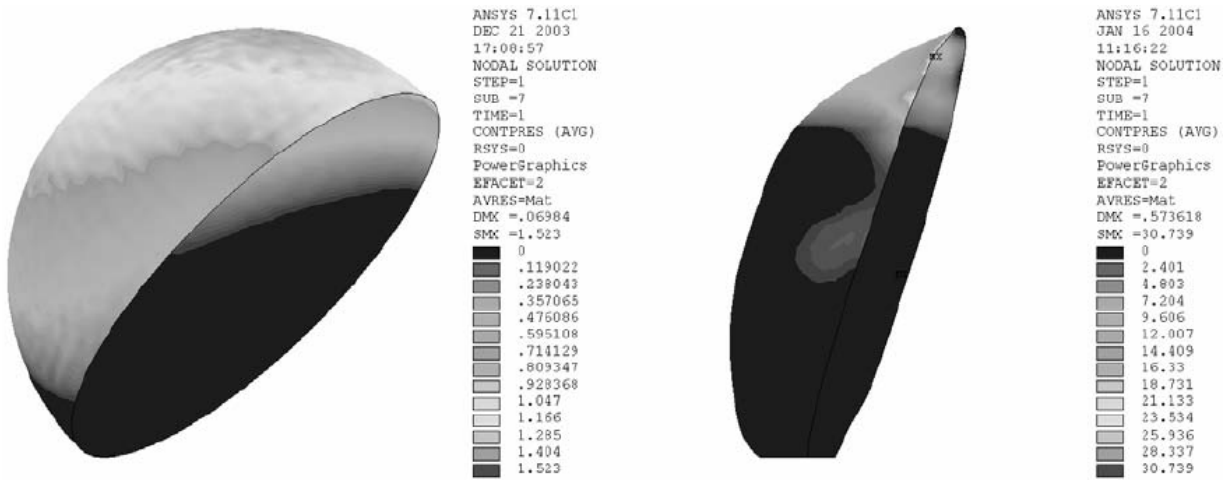
Figure 21 - Normal Femoral head (L) and Dysplastic Femoral head (R) [23]
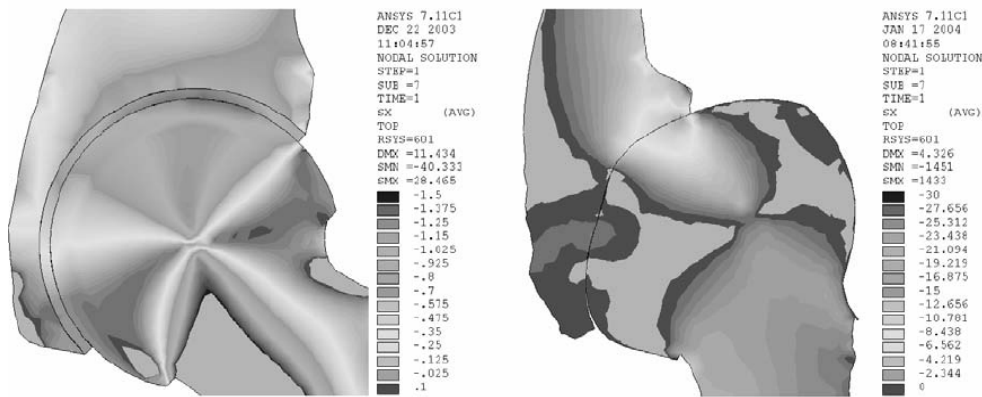
Figure 22 - Normal Hip Joint (L) & Dysplastic Hip Joint (R) [23]

The Iliopsoas Tendon in Hip Dysplasia and Other Conditions of the Hip

The iliopsoas tendon has been identified as an obstruction to reduction for infants with developmental dislocation of the hip[24]. However, the 3-dimensional orientation of the iliopsoas tendon in positions of flexion and abduction has not been previously reported. During closed reduction when the hip is in extension, the iliopsoas tendon causes an hour-glass constriction at the joint capsule, which may be demonstrated by arthrography. However, reduction is achieved with the hip in flexion and abduction, and in this position the iliopsoas tendon may not be an obstacle to reduction. Traction has been reported as a method to stretch contracted muscles, including the iliopsoas, prior to reduction[25].

With prolonged dislocation the hip capsule becomes narrowed between the femoral head and the acetabulum forming an hour-glass constriction. The iliopsoas tendon may contribute to the development of this constriction, but the question remains whether the iliopsoas tendon itself or the persistent capsular contracture prevents reduction when the hip is flexed [24; 26].

Successful arthroscopic reductions have been reported without release of the iliopsoas tendon [27]. In contrast, the iliopsoas tendon is released during open surgical procedures to increase joint exposure and decrease the tendency to re-dislocation when the hip is maintained in an extended position during the post-operative period [28].

The 3-dimensional orientation of the iliopsoas tendon may also have clinical relevance for musculoskeletal conditions and procedures other than hip dysplasia. In children with cerebral palsy, this tendon is released to prevent spastic hip dislocations[29], to relieve joint contractures[30], and to improve gait. Additionally, a better understanding of the position of the iliopsoas tendon may benefit conditions that involve structures in the vicinity of the acetabulum

such as snapping hip[31], labral lesions[32], and iliopsoas impingement following arthroplasty procedures[33].

Alpert, et.al., characterized the 3-dimensional anatomy of the iliopsoas tendon and its relationship to surrounding structures[32]. In otherwise healthy hips, the iliopsoas does not adhere to the hip capsule and is separated by a bursa. Alpert's study consisted of cadaver dissections with the hips in the neutral position without assessing anatomical relationships in various positions of flexion and abduction. Jacobson and Allen reported anatomical dissections of the iliopsoas tendon to study the pathophysiology of the snapping hip[31]. They noted that the iliopsoas tendon moves laterally when the hip is flexed and abducted, but their dissections did not evaluate dislocated hips.

The purpose of this part of the study was to determine the 3-dimensional orientation of the iliopsoas tendon in different combinations of hip abduction and flexion, in healthy and dislocated hips. A major goal of the study was to identify when the iliopsoas tendon may, or may not be an obstruction to the reduction of hip dysplasia. Our investigations were conducted using MRI and CT scan data, as well as computer modeling techniques to cross check, visualize and illustrate findings obtained in a cadaveric dissection.

Background and Significance

Overview

Hip dysplasia is very common in otherwise healthy infants. Severity ranges from mild instability to complete hip dislocation. The true incidence is difficult to quantify due to ethnic

and cultural differences combined with variations in diagnostic criteria. In Western cultures hip instability can be detected in 5-15% of newborns with 4 to 7 per thousand requiring treatment [34-39]. Approximately 1-2 children per thousand have complete dislocation of the hip at birth[37; 40]. When left untreated, mild dysplasia may lead to early hip joint arthritis while complete dislocations lead to life-long disability [41; 42]. In underdeveloped regions, hip dislocations may not be detected until children have reached walking age when a limp is noted. Correction of hip dislocation in the older infant often requires prolonged immobilization or surgery that may not be readily available in underdeveloped regions.

In spite of the common nature of this condition, there are numerous controversies surrounding the treatment of hip dysplasia in infants and young children. Bracing is usually effective in infants, but there are wide variations regarding the types of braces, indications for treatment, and duration of brace wear. Some methods of bracing may increase the risk of necrosis of the femoral head. Complete dislocations are less amenable to current bracing methods.

Several different braces have been recommended, however, there is disagreement regarding the use of a rigid orthosis versus a dynamic harness with straps that allows limited movement [43-45]. The Pavlik Harness, nevertheless, is the most widely used method for treating hip dysplasia in infants. Success rates of 95-100% have been reported in series that include patients with mild dysplasia [46-48], however, infants with complete dislocations have lower success rates when using the Pavlik Harness.

For infants younger than six weeks with complete dislocations the reported rates of success are only 64-85% [47; 49; 50], while infants with dislocated hips that are clinically

irreducible have an even higher failure rate with the Pavlik harness method, with success rates in this most severe group of patients ranging from 0-63% [50-53].

Additionally, avascular necrosis of the femoral head has been reported in 0-28% of patients treated with the Pavlik harness [43; 47; 49; 54], indicating that there is wide variation in success rates and risks associated with use of this device. Some of these variations may be due to inclusion of infants with mild hip dysplasia or hips that are irreducible at the time of initial diagnosis, however, when treatment with the Pavlik harness fails, patients will require either closed reduction with cast immobilization or open reduction.

Since there is wide variation in the rate of success with these methods for this group of patients, in addition to surgeon experience as a factor for success, other factors predictive of failure may well be identified using computer models to replicate the force and torque components generated on dysplastic hips during use of the Pavlik Harness, with the latter being the aim of this project.

Age and Dysplastic Condition Limitations of Current Treatment

The indicated age for Pavlik harness treatment is 0-6 months of age. Infants with dislocated hips that are clinically reducible are generally treated with braces that are applied in the outpatient setting [55-57], and the braces are worn for a patient-specific, indefinite time, until the hip stabilizes in a reduced position.

Objectives of This Study

Aim #1:

To identify fundamental mechanical characteristics of DDH treatment with the Pavlik harness.

Aim #2:

To identify the role of the Iliopsoas tendon in dysplastic hips, and determine the hip configurations in which this tendon becomes an obstruction to the treatment of the condition, as well as the hip configurations in which it does not pose an obstruction.

Aim # 3:

To develop and characterize an anatomy-based finite element and dynamics computer model of an infant hip that will simulate the physiological response of the hip due to the loads imposed by the Pavlik harness.

Aim # 4:

To utilize the anatomy-based finite element and dynamics computer model to study the effects of different anatomical and physical factors in the reductions of hip dysplasia, as well as investigate alternative treatment approaches to the condition.

Aim # 5:

To further develop this computational model to make possible the systematic determination of the optimum Pavlik harness load components, necessary to successfully vector the femoral heads into their correct physiological position in the acetabula, while maintaining hip reduction during the entire length of the treatment in a case, and patient-specific manner, and in this way allowing physicians to make more realistic and beneficial decisions when developing treatment plans.

CHAPTER TWO: METHODS

A 3D dynamic computer model was developed to simulate treatment of two severities of hip dysplasia with the Pavlik harness.

Model Definition

To construct the model, we used CT-scans of a 6 month-old female and the medical segmentation software Mimics (Materialise Inc., Plymouth, MI) to measure the geometrical features of the hip joint including acetabular and femoral head diameter, acetabular depth, and geometry of the acetabular labrum. The lower extremity was modeled by three segments: thigh, leg, and foot. The mass (Table 2) and the location of the center of gravity of each segment were calculated using anthropometry [58-61]. Calculations were based on the total body mass of a 6-month old female infant at the 50th length-for-age percentile [62].

Table 2: Masses of the segments of the lower extremity (Drillis and Contini, 1966)

Masses of segments of the lower extremity		
Total Body Mass (BM)	7.26 kg	
Segment	%BM	Mass
Thigh	9.46	0.69 kg
leg	4.2	0.30 kg
Foot	1.35	0.10 kg
Full leg	15	1.09 kg

Geometrical measurements and mass calculations were used to develop a dynamic computer model utilizing SolidWorks (Dassault Systèmes Simulia Corp., Providence, RI)

31

consisting of the pubis, ischium, acetabulum with labrum and femoral head, neck, and shaft (Figure 23), capable of simulating dislocated as well as reduced hips in abduction and flexion (Figure 24a-c). Only the right hip was modeled due to symmetry.
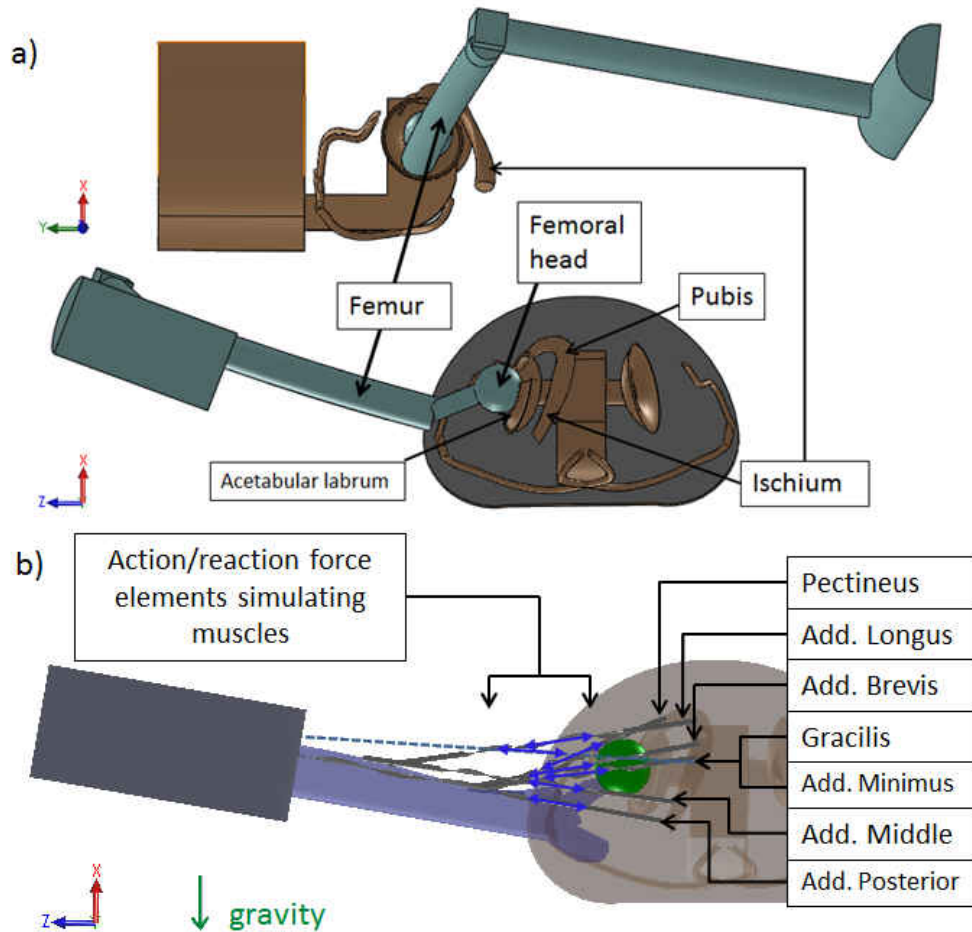
Figure 23- Three-dimensional dynamic computer model for simulations of hip dysplasia reductions. a) Hip and right leg assembly viewed laterally (topmost) and axially (middle). b) Hip and right leg assembly viewed axially, displaying modeled musculature.
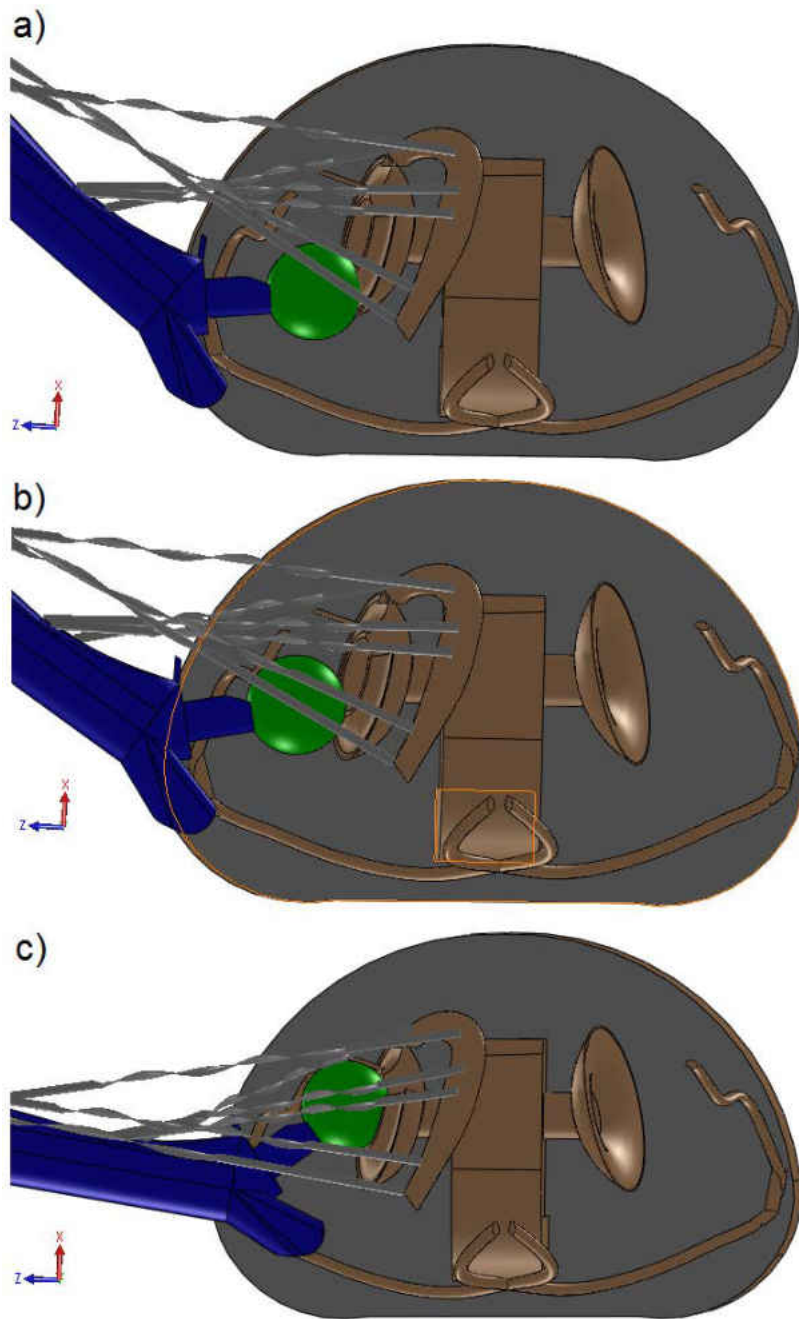
Figure 24 - Hip dislocation cases modeled: (a) full dislocation (Graf IV) with femoral head located posterior to acetabulum, (b) subluxated hip (Graf III) with the femoral head located over the posterior acetabular labrum, and (c) reduced hip.

The origin of the inertial Cartesian reference frame was fixed at the center of the right acetabulum (Figure 25). The femoral head was constrained to move in the X-Z plane. Hip rotations were constrained about the Z and X axes to account for the analogous constraints imposed by the anterior (flexor) stirrup strap (Figure 2) of the Pavlik harness, and to account for reaction moments imposed by possible anatomical structures not included to reduce complexity. Contact between the femoral head and the acetabulum was modeled as frictionless solid body contact.
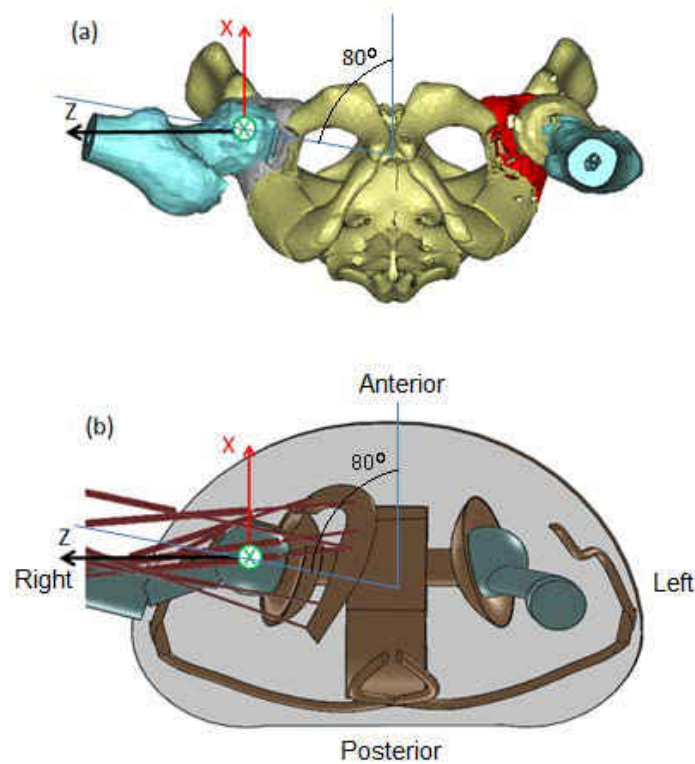
Figure 25 - Depiction of reconstructed anatomy and computer model: (a) CT-based three-dimensional hip reconstruction. (b) Simplified solid model with musculature. Y-axis of the right-handed coordinate system points normal to the page. Both models viewed in the in

Locations of origins and insertions of muscles were assigned by scaling adult male data [63] isotropically to match the proportions of the 6-month old infant, using the distances between acetabular centers as scaling parameters. The resulting scaling factor was 0.39 and the scaled muscle origins and insertions (Table 3) matched the expected model landmarks accurately.

Table 3: Coordinates of muscle origins and insertions scaled to fit 6-mo old female infant for Hip configuration: Zero abduction, zero flexion, and zero rotation. Unscaled data obtained from [63].

Scale: 0.39			Origin on Pelvis (mm)			Femoral Insertions (mm)		
			X	Y	Z	X	Y	Z
**	Iliopsoas		11.1	9.5	2.0	-0.8	-24.2	5.9
1	Pectineus		17.4	-1.2	-15.0	-1.6	-45.1	13.9
2	Adductor Longus		16.2	-12.3	-25.7	2.0	-80.8	10.3
3	Adductor Brevis		8.3	-17.8	-26.5	-0.8	-51.9	15.0
4a	Magnus	*Adductor Minimus*	2.8	-19.4	-24.2	-1.6	-49.1	15.8
4b		*Adductor Middle*	-12.3	-24.2	-17.4	2.0	-90.3	10.7
4c		*Adduct Posterior*	-19.0	-23.4	-13.5	0.4	-160.0	-12.3
5	Gracilis		4.0	-19.4	-26.9	-5.5	-171.9	-16.2

** Effect of the IIiopsoas tendon was studied separately

Muscle Modeling

Five anatomical muscles were considered to affect DDH reduction with the Pavlik harness: Pectineus, Adductor Brevis, Adductor Longus, Adductor Magnus, and Gracilis. The Adductor Magnus is a large triangular muscle with extensive femoral insertion; consequently, in the computer model this muscle was represented by three effective components following [63]: *Adductor Minimus, Adductor Middle, and Adductor Posterior*, corresponding to the proximal,

middle, and distal femoral insertions of the muscle, respectively. The computational model thus results in seven distinct muscle entities: Pectineus, Adductor Brevis, Adductor Longus, Gracilis, *Adductor Minimus, Adductor Middle,* and *Adductor Posterior.*

According to [64; 65] reductions of DDH with the Pavlik harness occur passively with muscle relaxation in deep sleep. The passive response of muscles to elongation is exponential [66-69]. We adopted the model by Magid and Hill in Equation (1), with constants in Table 4, to simulate the response of adductor muscles to elongation.

$$\sigma = \frac{E_0}{\alpha}(e^{\alpha(\lambda-1)} - 1) \qquad (1)$$

Table 4: Variables in Equation (1) and Equation (2) as defined by Magid (Magid and Law, 1985).

Variable definitions for Eq. (1) and Eq. (2)		
α	Empirical constant	4.28 ± 0.19
E_0	Initial elastic modulus	2.6 ± 0.25 (x10^3 N/m^2)
A	Cross sectional area	41 mm^2
λ	Muscle stretch	L / L_0

Where $\lambda = L / L_o$ is the stretch, L is the deformed length and L_o is the initial length. To obtain muscle tensions (T), we multiplied Equation (1) by an effective cross-sectional area, A=41 mm^2, approximated by dividing the volume of the Adductor Brevis muscle by its length determined from MRI data. The magnitude of this area is an intermediate value between that of the Pectineus and Adductor Longus. Given that the Adductor Magnus was discretized into three

effective component muscles, this area was used as a representative value for all modeled muscles.

The model was then calibrated by calculating a stiffening factor C that allowed the model to precisely replicate clinical observations in which healthy (non-dysplastic) infant hips are maintained in static equilibrium when infants are supine and the hips are placed in abduction and flexion, with slight infero-superior support to maintain flexion. We adopted 80° abduction and 90° flexion (Figure 25) as the "reference configuration."

For model calibration, unknown tensions in seven pre-stretched muscles (Pectineus, Gracilis, Adductor Brevis, Longus, *Minimus, Middle* and *Posterior*) were related as ratios to the tension of the adductor Brevis, which experiences the largest stretch (Table 5).

Table 5: Static equilibrium muscle tensions for a 6-month old infant hip at 80° abduction and 90° flexion. Li defines the length of the muscles in the natural position in the body.

Muscle	Initial muscle length**(L_0)	Stretch (λ) at 80° abduction, 90° flexion	Tension (N)
Pectineus	0.6 x Li	1.96	8.9
Adductor Longus	0.6 x Li	2.32	38.2
Adductor Brevis	0.6 x Li	2.54	97.8
Magnus *Adductor Minimus*	0.675 x Li	2.31	21.3
Magnus *Adductor Middle*	0.675 x Li	2.28	23.6
Magnus *Adductor Posterior*	0.675 x Li	1.91	6.2
Gracilis	0.675 x Li	1.92	26.7

** per Hill muscles are 25-40% stretched in their natural position in the body [69].

The Finite Element Method (FEM) software package NX Nastran (Siemens PLM Software, Plano, TX, USA) was employed to solve for the unknown tensions. For this FEM

solution, we used rigid bar elements (RBAR) to account for the femur, tibia and fibula (modeled as a single component), and foot. Due to the passive nature of reductions of DDH with the Pavlik harness [64; 65], the weight of the leg is the only driving force in the model. The weight of the leg was modeled as a point load of 10.7N pointed in the –X direction (Figure 23, Table 2), acting through the center of mass of the leg. All translations and rotations were constrained at the hip joint except rotation about the y-axis. Resolution of the force components along the lines of action of the muscles (Table 5) yielded the approximate muscle tensions necessary for static equilibrium at the reference configuration. These were then used to calculate a calibration constant resulting in a value of C=5.5 (Figure 26), yielding the final muscle model:

$$T = CA\frac{E_0}{\alpha}(e^{\alpha(\lambda-1)} - 1) \qquad (2)$$
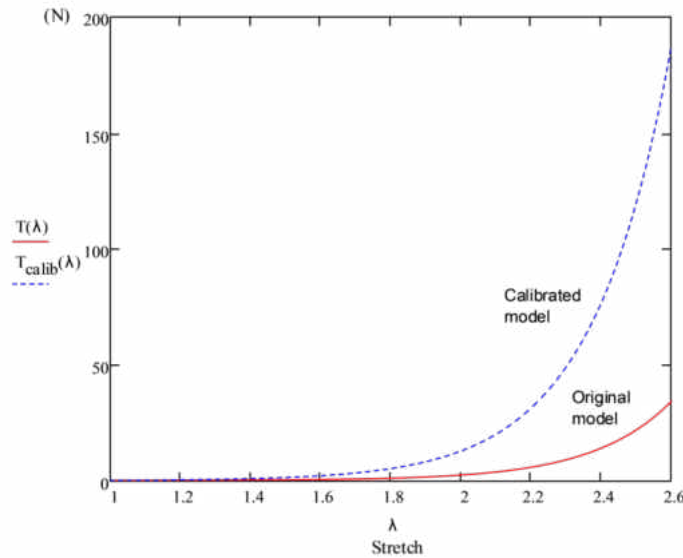
Figure 26 - Original muscle model (Magid and Law, 1985) and calibrated model.

Stiffening is attributed to a combination of unaccounted leg-supporting structures, difference in the density of elastic muscle fibers between muscles, and difference in mechanical

38

behavior between human and amphibian muscles. In the dynamic model, hip muscles were subsequently simulated using action/reaction force elements positioned between muscle origin and insertion points, following the non-linear constitutive equation provided in Equation (2).

Simulations

Simulations were carried out using the ADAMS dynamics module embedded in the software package SolidWorks, which numerically solved the set of coupled differential equations of motion [70]:

$$\underline{\underline{M}}\ddot{\underline{q}} + \beta\underline{\phi}_{\underline{q}}^{T} - \underline{\underline{A}}^{T}\underline{F}(\underline{q},\dot{\underline{q}}) = 0 \qquad (3)$$

subject to the natural constraints:

$$\underline{\phi}(\underline{q},t) = 0 \qquad (4)$$

where $\underline{\underline{M}}$ is the mass matrix of the system, $\underline{q}$ is the vector of generalized coordinates for the displacements, β is a Lagrange multiplier, $\underline{\phi}$ is the set of configuration and applied motion constraints, $\underline{\underline{A}}^{T}$ is the matrix that projects the applied forces in the $\underline{q}$ direction, $\underline{\phi}_{\underline{q}}$ is the gradient of constraints, and $\underline{F}$ represents the applied forces and gyroscopic terms of the inertia forces. In the computations, the Gear Stiff (GSTIFF) integrator was used, the Jacobian was updated at each time-step, 25 sublevel iterations were taken per time-step, and the initial, minimum, and maximum integrator step sizes were set to 1×10^{-4}, 1×10^{-7} and 1×10^{-2}.

Two severities of DDH were analyzed and simulated:

(1) Graf III subluxated hip: center of the femoral head lies on posterior rim of the acetabulum (Figure 24b).

(2) Graf IV fully dislocated hip: center of the femoral head is located posterior to the acetabulum and obstructed by the labrum (Figure 24a).

Magnitudes and directions of forces developed in each muscle were analyzed separately. First, we compared directional cosines of the lines of action of each muscle with those of resultant forces necessary to induce motion towards reduction. For condition (1) we evaluated the contributive components of muscle forces at 43°, 52°, 60°, 70°, and 80° of abduction. For condition (2) we evaluated components at 52° and 70° of abduction. For each DDH severity studied we reported findings as the percentage contribution of each muscle force in the direction necessary to affect reduction.

Reduction simulations were carried out by positioning the hips in configurations (1) and (2) as initial conditions, and solving the dynamic response of the system until equilibrium was reached. We defined successful reductions as conditions in which the femoral head slid into the acetabulum, and concentric reduction was maintained throughout the solution (Figure 24c) as the leg reached equilibrium.

Three-Dimensional Orientation of the Iliopsoas Tendon in Healthy and Dysplastic Hips: Evaluation

We studied the straight-line path of travel of the Iliopsoas tendon as it departed from its last point of contact on the bony pelvis towards its insertion point in the femur, neglecting tendon

volume, to determine possible interference to reductions of hip dysplasia. For this study we conducted a cadaveric dissection and studied the three-dimensional orientation of the iliopsoas tendon in healthy and dysplastic hips independently. Subsequently we replicated our findings in a computer model for better analysis and visualization. For healthy hips, we analyzed the path of travel of the iliopsoas tendon in the following hip configurations: 0° abduction and 0° flexion; 0° abduction and 15°-20° flexion; 45° abduction and 0° flexion; 45° and 15°-20° flexion. For dysplastic hips, we analyzed the path of travel of the iliopsoas tendon in the following hip configurations: 0° flexion and 0° abduction; 0° flexion and 90° abduction; 0° flexion and >90° abduction; 50° flexion and 90° abduction.

Cadaveric Observations and Analysis of the Path of Travel of the Iliopsoas Tendon

The iliopsoas tendon of a cadaveric specimen belonging to an 87-year old female was exposed using a wide Smith-Petersen extended anterior surgical approach. The sartorius was released and the rectus femoris muscle was exposed to allow visualization of the joint capsule and iliopsoas tendon with particular care to preserve the structures and muscles surrounding the iliopsoas. The iliopsoas muscle and tendon were noted to cross the pelvic brim in the groove between the anterior inferior iliac spine laterally and the pectineal eminence medially. At no point was the iliopsoas muscle or tendon fixed to the groove or to the anterior hip capsule.

In order to improve abduction in the reduced position and allow for hip dislocation, the adductor muscles were released medially through a separate incision. With the cadaver remaining in the supine position the femur was positioned systematically into different configurations while the condition and positioning of the iliopsoas tendon were noted and

recorded using high definition photography and video for each configuration. The configurations studied while the femoral head was reduced included the following: 0° abduction & 0° flexion, 0° abduction & $15\text{-}20^o$ flexion, 45° abduction & 0° flexion, and 45° abduction & $15\text{-}20^o$ flexion.

Next, the hip joint capsule was incised circumferentially to improve mobility, but the relationship of the iliopsoas muscle and tendon were preserved. The hip was again systematically placed into various configurations while the state and positioning of the iliopsoas tendon were documented and photographed for each position. The hip was then dislocated with release of the ligamentum teres, and the movements were repeated with the dislocated femoral head. The following configurations were studied: 0° abduction & 0° flexion, 0° abduction & 90° flexion, 0° abduction & $>90^o$ flexion, and 50° abduction & 90° flexion.

Computer Model of the Hip, Femur and Iliopsoas Tendon

The 3-dimensional (3D) computer model of a human hip and right femur was generated by reconstructing CT-scan data of a 14-year old female using the medical segmentation and processing software packages Mimics and 3-matic (Materialise Inc, Plymouth, MI). The reduced and dislocated hip (Graf IV) configurations studied in the cadaveric dissection were then replicated in the computer model. For reduced hips, the hip configurations replicated in the computer model were 0° abduction & 0° flexion, and 45° abduction & 0° flexion. Modeled hip configurations for dislocated hips were 0° abduction & 0° flexion, 0° abduction & 90° flexion, and 50° abduction & 90° flexion. For each hip configuration the psoas tendon was then digitally added using computer-aided modeling techniques to study and illustrate its path of travel. The

tendon traveled directly to the lesser trochanter as expected[71], and the origin correlated well with that reported by Dostal and Andrews (1981), who completed a cadaveric-based biomechanical model of hip musculature, and assigned a fictitious origin to the iliopsoas tendon at the last point of contact as it wrapped around the anterior bony pelvis[72].

CHAPTER THREE: RESULTS

Biomechanics of Hip Dysplasia Treatment with the Pavlik Harness

The Pavlik harness maintains hips abducted and flexed, and we approximated this position as 80° of abduction and 90° of flexion. We found that: (1) the psoas tendon is relaxed and is likely not an obstruction to reduction for any abduction angle while the hips are flexed to 90°. This holds true for Graf III and Graf IV dislocations, and the reference configuration; (2) the psoas tendon obstruction to hip reduction only occurs for hips extended beyond approximately 45° as the tendon tightens upon extension, and its straight-line path interferes with the joint capsule.

Inducing a Graf III subluxation, while maintaining the length of the Pectineus muscle constant, resulted in a reduction of 28° in abduction angle, which agrees with our clinical observations and those of [64; 65], providing a validation of our model. A successful dynamic reduction simulation was carried out indicating that Graf III subluxations can be reduced by the Pavlik harness. To study the mechanisms of reduction we considered (a) the magnitudes and (b) directions of muscle tensions. Tension magnitudes are functions of stretch (Figure 26), however it should be noted that tension values are affected by uncertainty in cross sectional area, and that muscles are 25-40% pre-stretched from the natural length (L_i) in the body [69]. The initial lengths (L_o) found to best suit the model were 0.60 x L_i for the Pectineus, Adductor Brevis and Adductor Longus, and 0.675 x L_i for the Gracilis and the effective components of the Adductor Magnus (*Adductor Minimus, Middle, and Posterior*).

44

Further insight is gained by comparing the stretch of muscles in healthy hips with those observed in dysplastic hips of Graf III, and Graf IV (Table 6). The Adductror Brevis has the largest stretch, hence tension, followed by the Adductor Longus and *Adductor Minimus,* depending on DDH severity.

Table 6: Comparison of muscle stretch values between reference hip configuration, Graf III, and Graf IV severities of hip dysplasia.

Muscle Stretch (λ)			
Muscle	Reference configuration	Graf III	Graf IV
Pectineus	1.96	1.96	1.96
Adductor Longus	2.32	2.23	2.21
Adductor Brevis	2.54	2.58	2.55
Adductor Minimus	2.31	2.4	2.11
Adductor Middle	2.28	2.36	2.05
Adductor Posterior	1.91	1.98	1.73
Gracilis	1.92	1.85	1.68

Examination of directional components of muscle tension upon inducing Graf III subluxation reveals that the Gracilis, *Adductor Middle,* and *Adductor Posterior* contribute negatively to the reduction with the Pavlik harness (Table 7), and that the percent constructive contribution of the muscles studied increases in direct proportion with abduction angle (Figure 27) which may explain observations by different authors of reductions occurring during loss of muscle tone while in deep sleep [64; 65].

Table 7: Percent directional contributions of muscle tensions in the direction of reduction - Graf III.

Percent directional contributions of muscle tensions - Graf III						
	Abduction Range (degrees, measured from sagittal)					contribution order
	42.7	52.2	60	70	80	
Pectineus	28.1%	38.7%	46.3%	55.5%	63.9%	1
Add Longus	-3.0%	10.1%	19.7%	31.6%	42.8%	4
Add Brevis	10.6%	20.4%	29.1%	38.9%	48.2%	2
Add Minimus	4.7%	15.7%	23.9%	34.2%	44.0%	3
Add Middle	-32.6%	-19.3%	-9.1%	4.4%	17.8%	5
Add Posterior	-44.6%	-30.2%	-19.0%	-3.9%	11.3%	6
Gracilis	-50.32%	-36.60%	-25.18%	-10.60%	4.00%	7
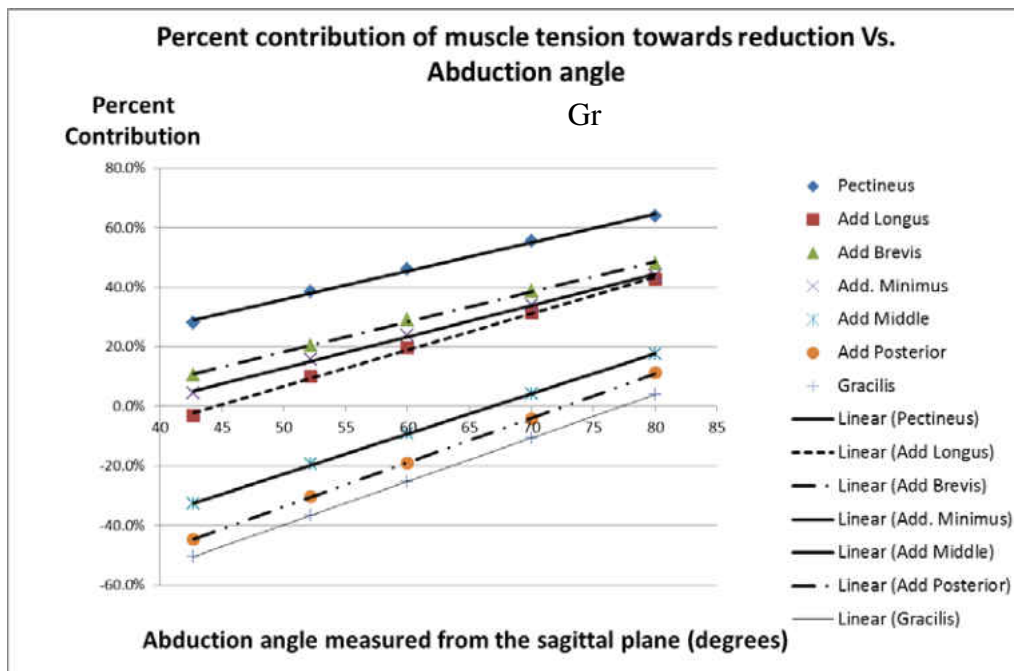
Figure 27 - Percent contribution of muscle tension towards reduction vs. abduction angle - Graf III.

Results in Table 7 indicate that the Pectineus, although less tense than other muscles in the Pavlik harness position, exhibits the highest component of pull in the direction of reduction (towards the center of the acetabulum) based on the line of action of its force, and thus helps effect and maintain reduction. This was later confirmed with a dynamic numerical simulation which successfully reduced the dislocation. Reduction was not achieved upon numerically suppressing the Pectineus.

Inducing a Graf IV type dislocation maintaining constant Pectineus muscle length resulted in a decrease in abduction of 13.7°. Simulation results indicate that reductions from dislocations of type Graf IV are unlikely to occur by Pavlik harness treatment, since the tensions of all muscles contribute negatively to the direction of the motion necessary for reduction (Table 8).

Table 8: Percent contribution of muscle tensions in the direction of reduction - Graf IV.

Percent directional contribution of tensions - Graf IV			
	Abduction angle		Contribution
	52.3°	70°	order
Pectineus	-42.9%	-29.7%	1
Add Longus	-64.8%	-52.2%	4
Addr Brevis	-53.5%	-42.1%	2
Add Minimus	-57.3%	-45.7%	3
Add Middle	-77.7%	-67.9%	5
Add Posterior	-86.5%	-77.3%	6
Gracilis	-91.3%	-84.0%	7

Based on origin and insertion points, muscles are shorter in a Graf IV dislocation than in a reduced hip. Since muscles tense when their length is increased from equilibrium, energy, hence traction to overcome muscle tension is necessary to bring the femoral head over the

posterior labrum for reduction. Furthermore, for Graf IV dislocations the directional contributions of the muscles also increased in direct proportion with increasing abduction angle (Figure 28), but abduction alone is insufficient to turn the detrimental directional cosines of the tensions into beneficial components, hence, reduction did not occur.
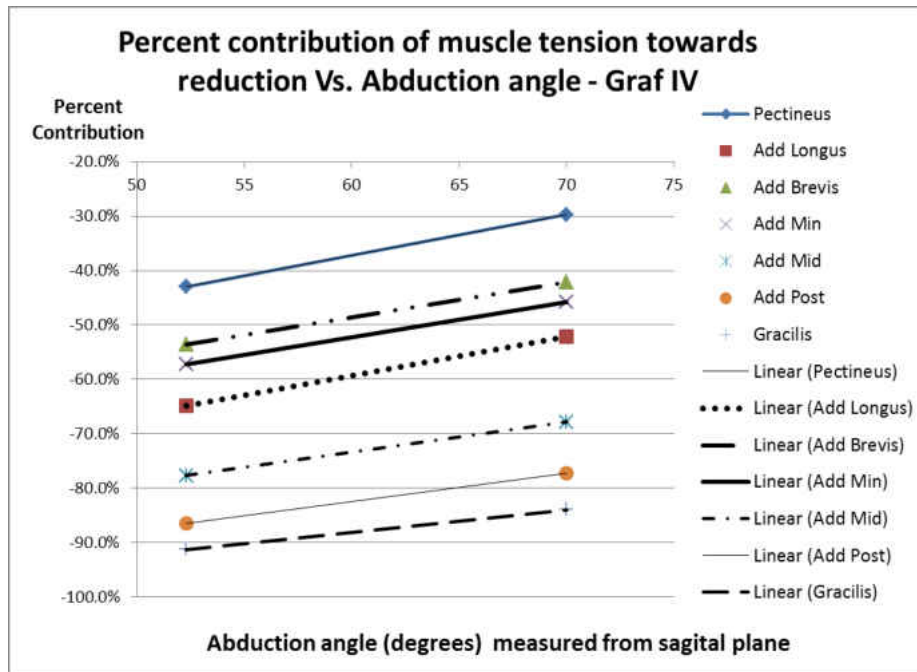
Figure 28 - Percent contribution of muscle tension towards reduction vs. Abduction angle - Graf IV.

Three-Dimensional Orientation of the Iliopsoas Tendon in Healthy and Dysplastic Hips:

Findings

For ease of visualization, the illustrations on this article contain the labels anterior (A), posterior (P), medial (M), lateral (L), superior (S), and inferior (I).

Results for the non-dysplastic hips were determined with the femoral head reduced in the anatomical position.

Position of 0° Abduction & 0° Flexion

In this position, the iliopsoas tendon wrapped over the anterior joint capsule in a highly taut manner. There was therefore no clearance between the tendon and the anterior capsulolabral complex (Figure 29, Figure 30); hence, any procedure requiring retraction of the tendon or exposure of the anterior joint capsule in this hip configuration would be enhanced by iliopsoas tendon release.
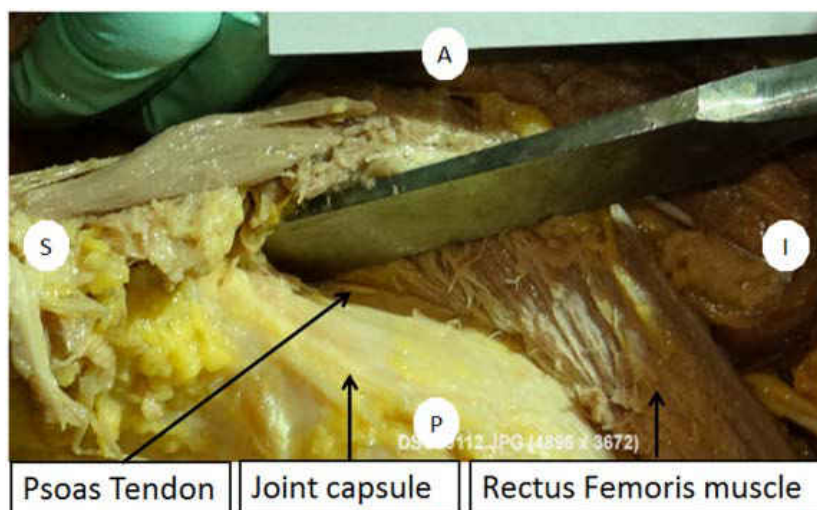
Figure 29 - Iliopsoas tendon wrapping tightly over the anterior joint capsule in 0° Abduction & 0° Flexion
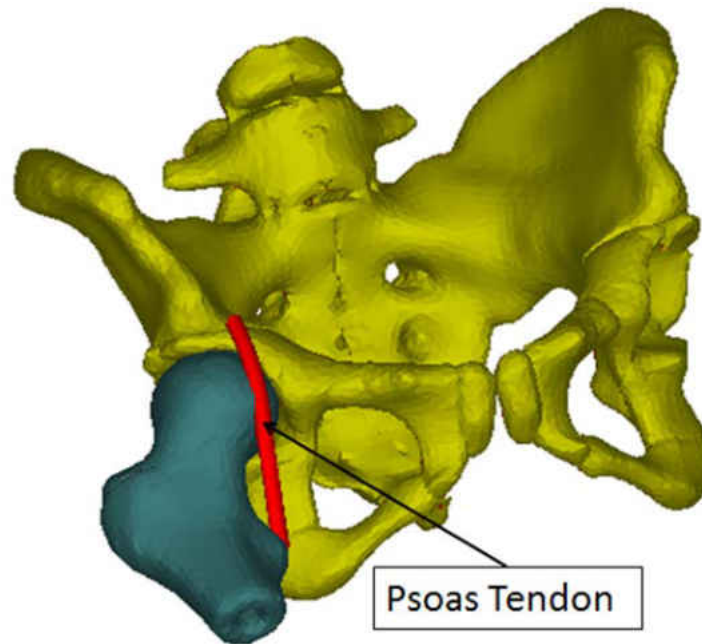
Figure 30 - Computer reconstruction of the iliopsoas tendon wrapping tightly over the anterior

joint capsule in 0° Abduction & 0° Flexion

Position of 45° Abduction & 0° Flexion

As the hip was maintained in extension but abducted from 0°to 45°, the iliopsoas tendon remained in contact with the anterior joint capsule, pressing tightly against the anterior capsulolabral complex at all times (Figure 31, Figure 32). The tension in the tendon at 45° abduction was judged by palpation to be qualitatively similar to the tension prior to abduction. It was also noted that the tendon was not fixed to the pelvic brim and moved laterally. This was also observed in the computer reconstruction of this configuration.
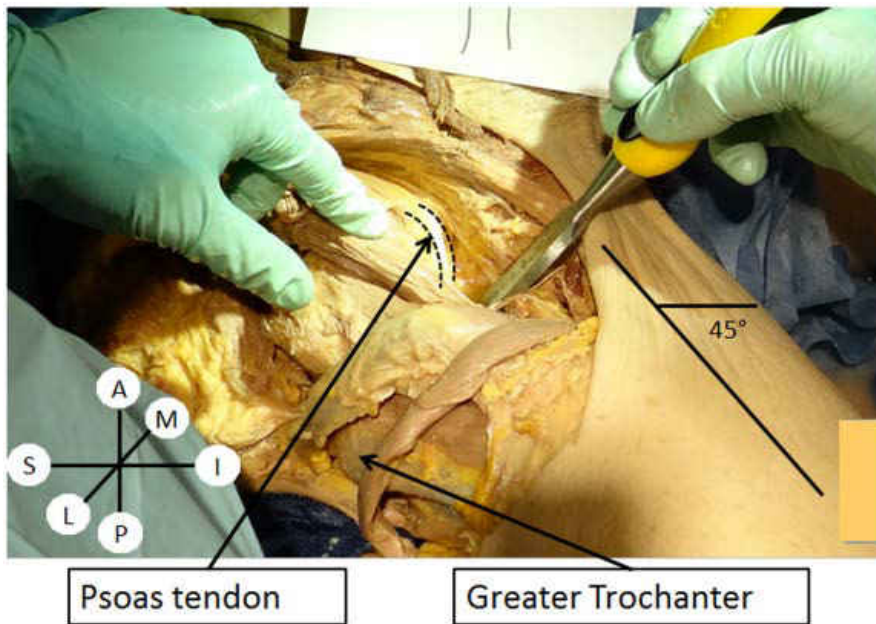
Figure 31 - Iliopsoas tendon wrapping tightly around anterior joint capsule in 45° Abduction &
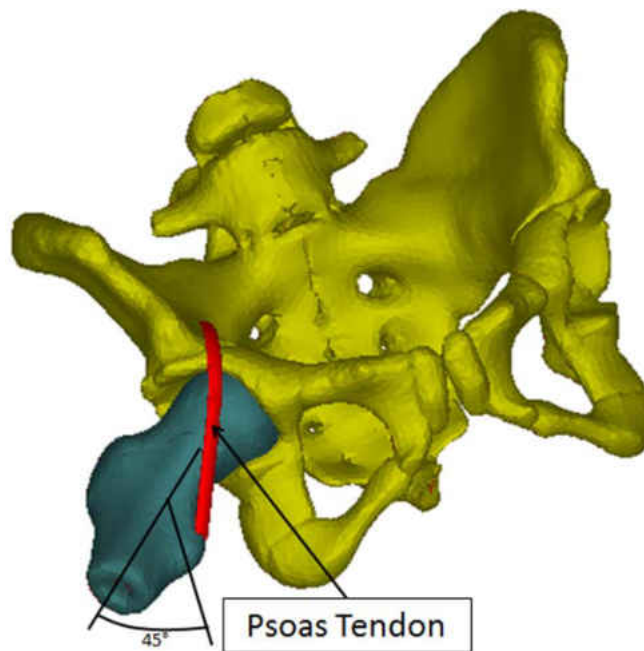
0° Flexion

Figure 32 - Computer reconstruction of iliopsoas tendon wrapping tightly around anterior joint

capsule in 45° Abduction & 0° Flexion

Position of 0° Abduction & 15-20° Flexion

In this position, the iliopsoas tendon did not interfere with the femoral head and joint capsule. The tendon was not fixed to the anterior hip capsule or to the pelvic brim, but was mobile with filamentous tissues between the iliopsoas and the joint capsule. Tension in the iliopsoas tendon began to relax shortly after flexion commenced, and slight clearance between the tendon and the anterior capsulolabral complex was identified. The flexion angle at which clearance between the iliopsoas tendon and the joint capsule first became noticeable was approximately 15°.

Position of 45° Abduction & 15-20° Flexion

Maintaining 45° abduction while flexing the hip to approximately 15° produced definite relaxation of the iliopsoas tendon, followed by the development of a palpable gap between the tendon and the hip joint capsule. Further flexion to approximately 90° while maintaining 45° abduction was obtained by releasing the posteromedial joint capsule through a 5 cm capsular incision along with release of the adductor muscles. This position demonstrated that the tendon fully relaxes and may be retracted to a limited extent without the necessity of a release if partial exposure of the anterior joint capsule is desired.

Dislocated Hips

Major changes in the positioning of the iliopsoas tendon were found after the joint capsule was circumferentially incised and the hip was dislocated. These findings were confirmed and illustrated independently using the computer model.

Position of 0° Abduction & 0° Flexion with hip dislocated

In this configuration the femoral head was noted to be superior to the acetabulum and the iliopsoas tendon was found to be taut and blocking visualization of the joint. Dissection findings and three-dimensional computer modeling of the iliopsoas tendon showed that the tendon path of travel crosses in a straight-line fashion between its origin and insertion such that the tendon sets between the femoral head and the acetabular opening (Figure 33, Figure 34). In this position the dysplastic hip capsule would assume an hour-glass constriction configuration; however, the cadaver dissection demonstrated interposition by the tendon where the capsule had been incised instead of the expected hour-glass constriction.
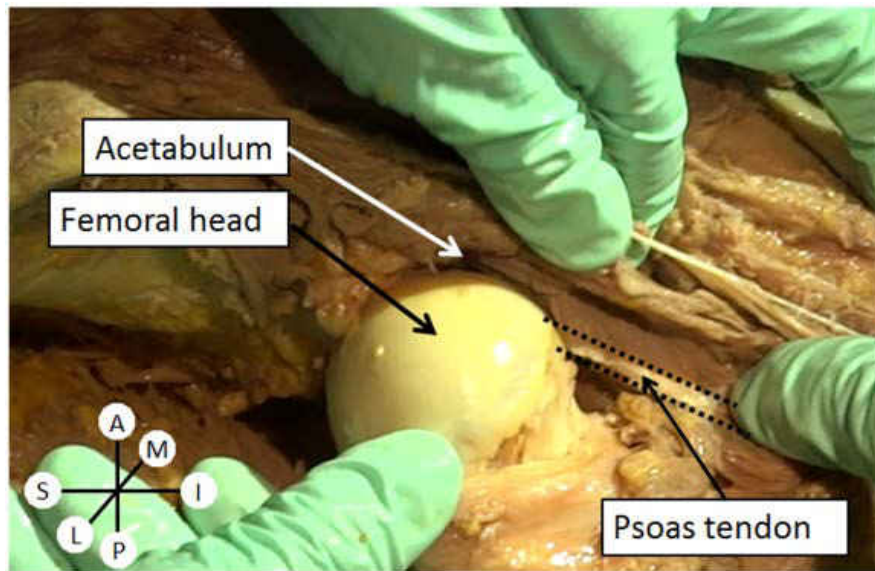
Figure 33 - Dislocated hip in 0° Abduction & 0° Flexion illustrating the path of travel of

the iliopsoas tendon medial to the femoral head, presenting as an obstacle between the femoral

head and the acetabulum
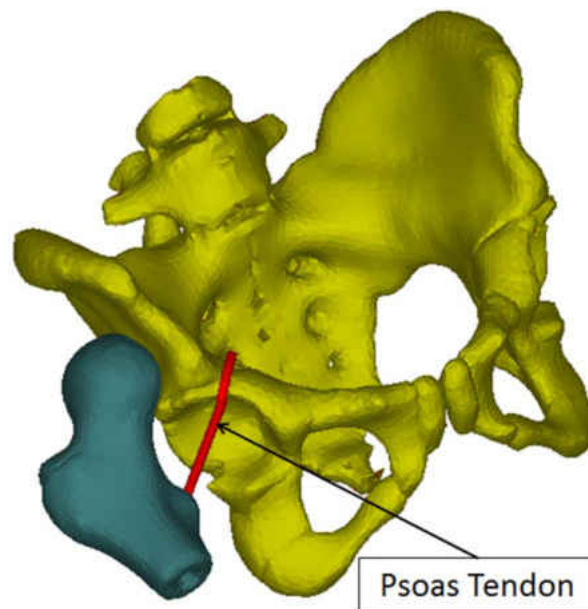
Figure 34 - Computer reconstruction of the iliopsoas tendon presenting as an obstacle

between the femoral head and the acetabulum in 0° Abduction & 0° Flexion in a dislocated hip

<u>Position of 0° Abduction & 90° Flexion With Dislocated Hip</u>

Upon inducing flexion, the femoral head moved from superior to the acetabulum to a position that was posterior and superior to the acetabulum. With further flexion, the femoral head moved in an inferior direction.

Simultaneously, during hip flexion the iliopsoas tendon moved more anterior and superior, becoming slightly, but not fully relaxed, as the femoral head rotated posterior to the tendon and acetabulum. The iliopsoas tendon cleared the acetabulum as hip flexion reached 90°, in which case the tendon was positioned at the superior margin of the acetabulum and anterior to the hip capsule tracing a line between the anterior inferior iliac spine and the insertion on the lesser trochanter, which was now anterior to the femoral head (Figure 35, Figure 36).
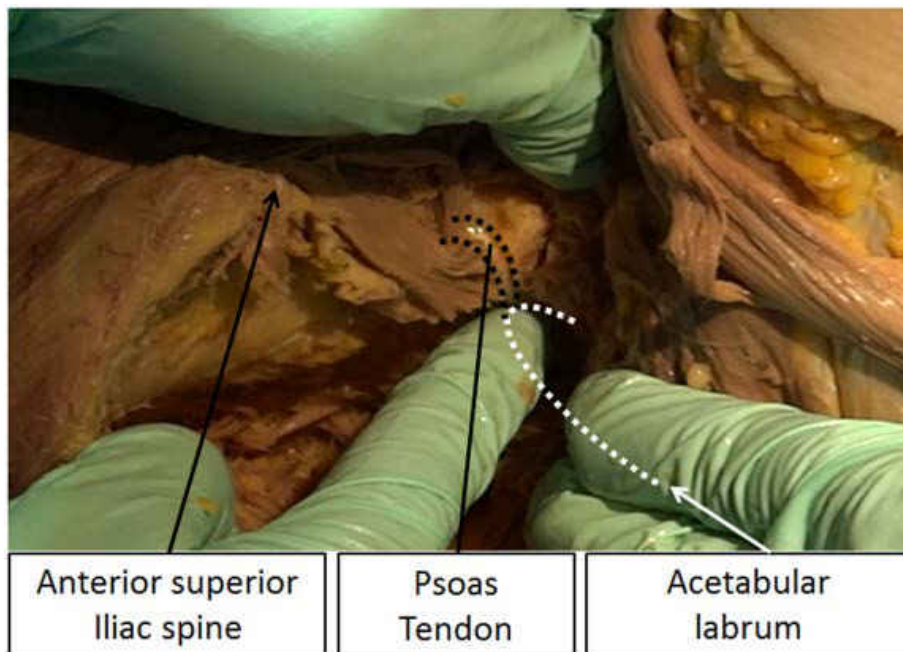
Figure 35 - Dislocated hip in 0° Abduction & 90° Flexion illustrating the path of travel of the iliopsoas tendon at the superior margin of the acetabulum.

55
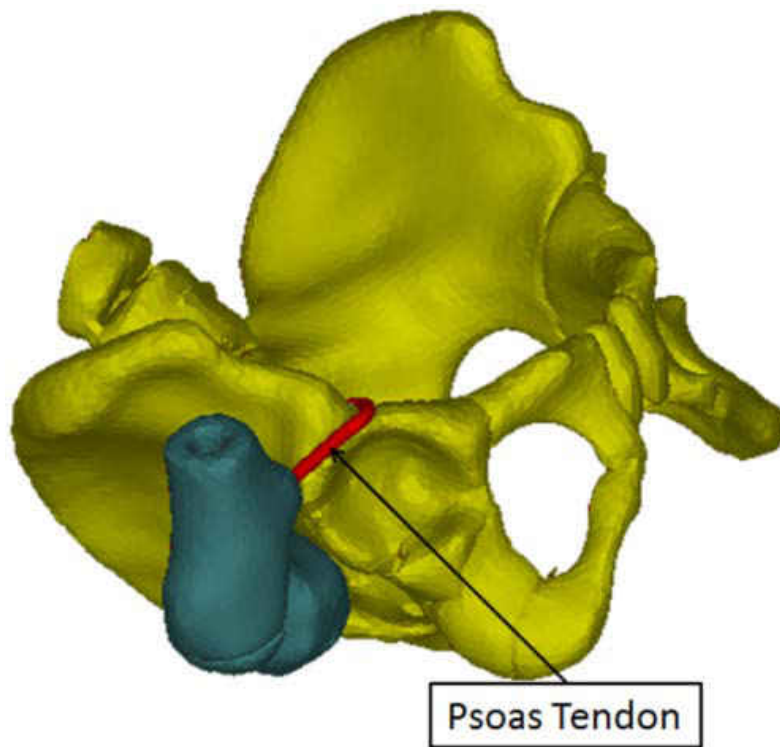
Figure 36 - : Computer reconstruction of the iliopsoas tendon anterior and superior to the

acetabulum and at the acetabular margin in 0° Abduction & 90° Flexion with a dislocated hip

Position of 0° Abduction & Flexion >90° (Hyperflexion)

Hyperflexion of the hip with no abduction resulted in further relaxation of the iliopsoas

tendon, along with displacement to a region superior to the acetabulum and fully clear of it.

Position of 50° Abduction & 90° Flexion

In this position the iliopsoas tendon remained superior to the acetabulum in any position

of abduction from 0° to 50° when the femoral head was posterior and superior to the acetabulum

(Figure 37).
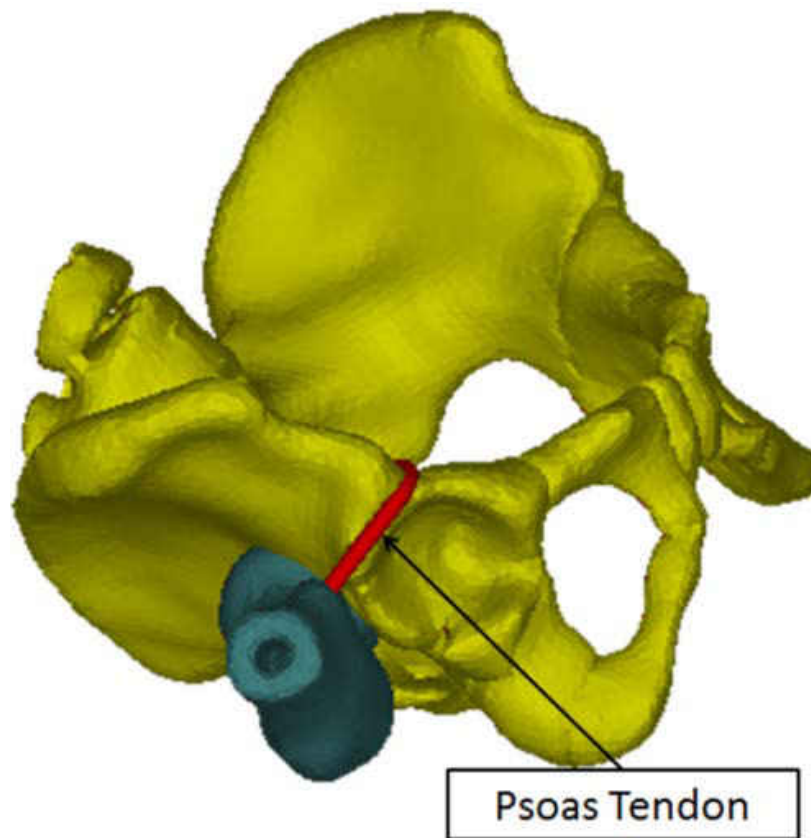
Figure 37 - Computer reconstruction of the iliopsoas tendon clear of the hip joint in abduction

and flexion in a dislocated hip

Additionally, the tendon remained slightly taut with flexion and abduction when the femoral head was posterior and superior to the acetabulum. The tension in this position was significantly smaller than that experienced by the tendon when the dislocated hip was in extension.

With the femoral head posterior to the acetabulum, the iliopsoas tendon rested on the anterior hip capsule while the hip was in 50° of abduction. Abduction beyond 50° was not evaluated in the cadaver or with the computer model.

CHAPTER FOUR: DISCUSSION

Biomechanics of Hip Dysplasia Treatment with the Pavlik Harness

Our findings indicate that the psoas tendon does not obstruct reduction when the hip is in flexion, which is the position of reduction in the Pavlik harness, and that of closed reductions with cast application. However, this tendon tightens and crosses anterior to the hip capsule upon hip extension becoming an obstruction to reduction. Releasing this tendon may only be necessary when reductions are sought with the hips extended, as in open reductions. Per the medial approach for open reduction of the hip, when the hip is extended, the iliopsoas muscle is taut, and released for greater surgical visibility of the capsule. Conversely, the "human position" (flexion and slight abduction) is recommended for closed reductions, and we found the Iliopsoas relaxed in this position. [73] reported arthroscopic reductions in the "human position" without iliopsoas release.

Although the Pectineus is significantly less taut in abduction and flexion, it was found to have a favorable line of action towards reduction. Conversely, the Gracilis and the portion of the Adductor Magnus of distal femoral insertion (*Adductor Middle and Adductor Posterior*), develop components of tension that oppose the direction desired for reduction. When the femoral head lies posterior to the acetabulum, these muscles pull the femoral head further posteriorly, trapping it in this location. This implies that traction is necessary to overpower the detrimental components of tension of these muscles when the hip is fully dislocated (Graf IV). Another avenue to overcome this could be the surgical release of these muscles, or alternative methods for closed management [74]. Hence, novel procedures that combine various techniques, in

addition to the possible artificial activation of the Pectineus muscle, may enhance treatment and contribute to successful reductions for hips that are irreducible with the Pavlik harness.

Based on our findings, reduction of higher degrees of dysplasia can be considered to take place as two distinct, consecutive events (Figure 38), and muscles act distinctively in each phase:

(a) Release phase: The femoral head is brought from a region posterior to the acetabulum to a region over the perimeter of the labrum.

(b) Reduction phase: follows the release phase and the femoral head is pulled into the acetabulum from a region over the perimeter of the labrum.
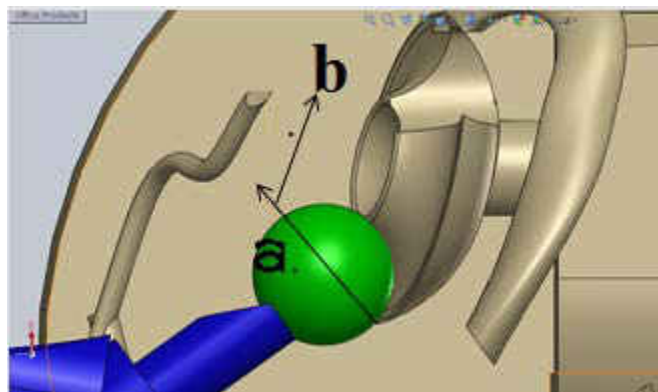
Figure 38 - Simplified model depicting the directions of necessary motion to complete the (a) Release and (b) Reduction phases of the mechanism of reduction of hip dysplasia.

In (a) the femoral head is released from external resistances constraining its movement such as it being trapped behind the acetabulum, the Piriformis muscle resisting its movement, or other resistive factors. (b) follows when the Pectineus muscle, due to its directional advantage, and the adductors (primarily the Adductor Brevis), take over and pull the femoral head into the

59

acetabulum. Acetabular geometry and the tension in the portion of the Adductor Magnus of distal femoral insertion help maintain concentric reduction.

Suzuki (1994) describes three degrees of hip dysplasia and states that the greatest severity, when the femoral head center lies posterior to the labrum of the acetabulum, requires traction for reduction. This is supported by our computational model: traction, referred to by Suzuki, is a method to free the femoral head from constraints, hence manually executing a release phase. Our findings, which correlate with previous observations, lead us to conclude that for hip dysplasia of greater severity (Graf IV), the release phase is highly unlikely via the Pavlik harness alone. Traction, surgical release of the distal adductors and/or a different treatment avenue is therefore required.

Three-Dimensional Orientation of the Iliopsoas Tendon in Healthy and Dysplastic Hips:

Findings

The position of the iliopsoas tendon during joint movement has implications for several musculoskeletal conditions including closed reduction of the dislocated hip, the snapping hip, labral lesions, and impingement following hip arthroplasty procedures. The results of this study confirm that the iliopsoas tendon is relaxed when the hip is flexed and it moves laterally at the pelvic brim when the hip is abducted in the flexed position[31]. When the hip is extended, the tendon is taut and presses against the anterior capsulolabral complex as noted by previous authors[31; 32]. Abduction and adduction with the hip extended allows the tendon to move over the joint capsule. This may produce snapping or impingement if the femoral head is prominent,

when hip replacement components are prominent following total hip arthroplasty, or when the anterior acetabulum is deficient.

Correspondingly, the iliopsoas tendon is reported to be the cause of the "internal" snapping hip syndrome, or coxa saltans, which "originates from a taut iliopsoas tendon that snaps across bony prominences when the hip is extended from a flexed position."[75] The clinical diagnosis is made when a painful snap is produced by extending, adducting, and internally rotating the hip from a flexed, abducted, externally rotated position[76]. The exact location of the snapping is uncertain. Some authors have suggested that the tendon snaps over the iliopectineal eminence although there is little documentation to support that opinion. In contrast, ultrasonography and anatomical dissections have suggested the snap is produced when the iliopsoas tendon moves over the prominent femoral head and anterior hip capsule[31; 76]. The region where the iliopsoas tendon passes over the anterior capsulolabral complex is also the most common location for labral pathology in patients with hip dysplasia[77]. The results of this study support previous reports that suggest the movement of the taut iliopsoas tendon over the femoral head and anterior capsulolabral complex plays a role in labral pathology, and in the snapping hip[31; 32].

The results of this study also identified the position of the iliopsoas tendon when the hip is dislocated. While the hip is extended the iliopsoas tendon crosses the opening of the vacant acetabulum and tightly constricts the anterior joint capsule. Flexion of the hip to 15°-20° begins to relax the tendon, and flexion of the dislocated hip to 90° moves the tendon against the anterior inferior iliac spine such that the tendon is superior to the opening of the acetabulum and does not constrict the hip capsule or limit the potential for closed reduction in that position. The iliopsoas tendon remains relaxed and proximal to the acetabulum when the hip is abducted in 90° of

flexion, thus it is unlikely that the iliopsoas musculotendinous unit is an obstacle to closed reduction when the hip is flexed and abducted, with the femoral head positioned at the level of the acetabulum.

The finding that the iliopsoas may not interfere with closed reduction of developmental dislocation of the hip is consistent with descriptions of obstacles to reduction reported in studies of hip arthrography during closed reduction. The principal obstacles to reduction have been identified as the limbus, capsular contracture and intra-articular anatomy of ligaments, fat and fibrocartilage [26; 78-80].

It should be noted that we are reporting findings of a study in which the iliopsoas tendon was not adherent to the hip joint capsule. One weakness of this study is that the iliopsoas tendon may be adherent to the joint capsule in longstanding cases of hip dislocation. Pathological adherence of the iliopsoas tendon could contribute to capsular constriction. In these cases, adherence of the iliopsoas tendon would present an obstacle to reduction, requiring the release of the tendon irrespective of flexion angle. Ishii et al. correlated arthrographic findings with operative findings in 51 patients ranging in age from 3 months to 4 years of age at time of treatment[26]. Five of these patients were found to have an iliopsoas tendon that was adherent to the hip capsule, although the age of the patients and the position of the hip was not reported during the surgical procedure. Eberhardt, et al, reported arthroscopic reduction after failed closed reduction in eight infants between the ages of 4 and 7 months[27]. His study found intra-articular obstructions along with capsular constriction, but none required release of the iliopsoas tendon to obtain reduction.

Release of the iliopsoas tendon is described as part of the procedure for open reduction of the dislocated hip through either the medial approach or through the anterior Smith-Peterson

approach. In describing the innominate osteotomy RB Salter noted that the reduced hip is stable in a position of abduction and flexion, but becomes unstable when it is brought back to the functional position of walking[81]. He recommended release of the iliopsoas in order to decrease the risk of re-dislocation rather than for the purpose of obtaining the initial reduction[28]. Salter's opinion is consistent with the findings of our dissections and computer model, however there may be cases where the iliopsoas tendon is adherent to the joint capsule and contributes to prevention of reduction as noted by Ishii, et.al [26].

Although release of the iliopsoas tendon is recommended during the surgical exposures for developmental dislocation of the hip, there may be long-term consequences. Bassett, et.al, evaluated the functional and anatomical changes in the iliopsoas muscle 4 to 9 years following release during open reduction for developmental dislocation of the hip[82]. These authors reported persistent atrophy of the iliopsoas muscle by MRI along with reduced maximum flexion torque during isokinetic testing of muscle strength. This finding along with the findings of our study suggest that preservation of iliopsoas may be worth considering as long as hip flexion and abduction are maintained long enough to gain additional stability after cast removal and prior to assuming the walking position.

In summary, the findings of this study suggest that the iliopsoas tendon is unlikely to be an obstacle to reduction during closed reduction for developmental dislocation of the hip. The iliopsoas musculotendinous unit is relaxed in all positions of flexion when the femoral head is at the level of the acetabulum. Due to the insertion on the lesser trochanter, the track of the tendon is slightly anterior to the hip capsule when the hip is in 90° of flexion and 0° abduction. In some cases the tendon may be adherent to the capsule where it could contribute to capsular constriction but this may be the exception rather than the rule. Improved methods of closed

reduction should focus on impediments to reduction other than the iliopsoas tendon such as tight adductor muscles, intra-articular obstructions and causes of recurrence such as abduction contractures and tension on the iliopsoas in the walking position as noted by Salter[81]. The findings of this study may also have relevance for conditions influenced by the iliopsoas tendon such as snapping hips, labral pathology and impingement following arthroplasty procedures.

CHAPTER FIVE: CONCLUSION

We created a three-dimensional computer model to simulate hip dysplasia reduction dynamics with the Pavlik harness. We identified five adductor muscles as key mediators in the prognosis of hip dysplasia (Pectineus, Adductor Longus, Adductor Brevis, Adductor Magnus, Gracilis), and found that reductions occur in two distinct phases: (a) Release phase and (b) Reduction phase. Results indicate that the muscles studied act distinctively in each phase and the mechanical effects of muscles vary with the severity of hip dislocation. For subluxated hips in abduction and flexion, the Pectineus, Adductor Brevis, Adductor Magnus of proximal femoral insertion, and Adductor Longus contribute positively to reduction, while the portions of the Adductor Magnus with middle and distal femoral insertion contribute negatively. Conversely, for fully dislocated hips, all muscles contribute detrimentally to reduction, explaining the need for traction to reduce Graf IV type dislocations. The Iliopsoas tendon was not found to affect reductions when hips are flexed, as during treatment with the Pavlik harness. Our model is consistent with clinical observations reported in the literature and may provide a means to determine modifications for treatment that could lead to new insights for non-surgical management of DDH by passive reduction with the Pavlik harness or similar devices.

APPENDIX: CURRENT RESEARCH

Development of an Anatomy-based FEM and Dynamics Computer Model

For additional studies of conditions of the hip, we developed an anatomy-based FEM and dynamics computer model consisting of the hip and femora of a 10-week old female infant. For its development we combined CT-scan data and muscle positional data from four different human subjects:

(1) 10-week old female infant

(2) 14-year old female

(3) 38-year old male (Visible Human Project, The National Library of Medicine)

(4) Adult Male of unknown age [63].

Various important regions of the infant hip are conformed of cartilage, and thus are difficult to visualize in CT-scans. For this reason we performed a 3-dimensional reconstruction of the CT-scans of a 14-year old female (2), and scaled it anisotropically to match the anatomical proportions of the 10-week old infant (1). Our scaling was performed by superposition of anatomical landmarks, namely anterior superior and posterior superior iliac spines, and acetabuli. Upon scaling the pubic and ischial rami of the scaled 14 year old female hip was found to trace a wider arc while all other landmarks matched well. This arc was manually modified to closely match the trace of the infant hip arc; we attribute the observed variation to the possible widening of female hips at puberty. Our resulting scaling factors were 0.35, 0.32, and 0.32 in the X, Y, and Z directions respectively.

To generate the right femur, CT-data from the Visible Human Project (3) was scaled anisotropically to match the femur size of the 10-week old female (1), according Standards in Pediatric Orthopedics [83]. We used femoral head diameter and length between epiphyseal plates

as scaling criteria. This procedure yielded scaling factors of and 0.22, 0.25 and 0.23 in the X, Y and Z directions. Making use of symmetry, the right femur was mirrored to create a model for the left femur.
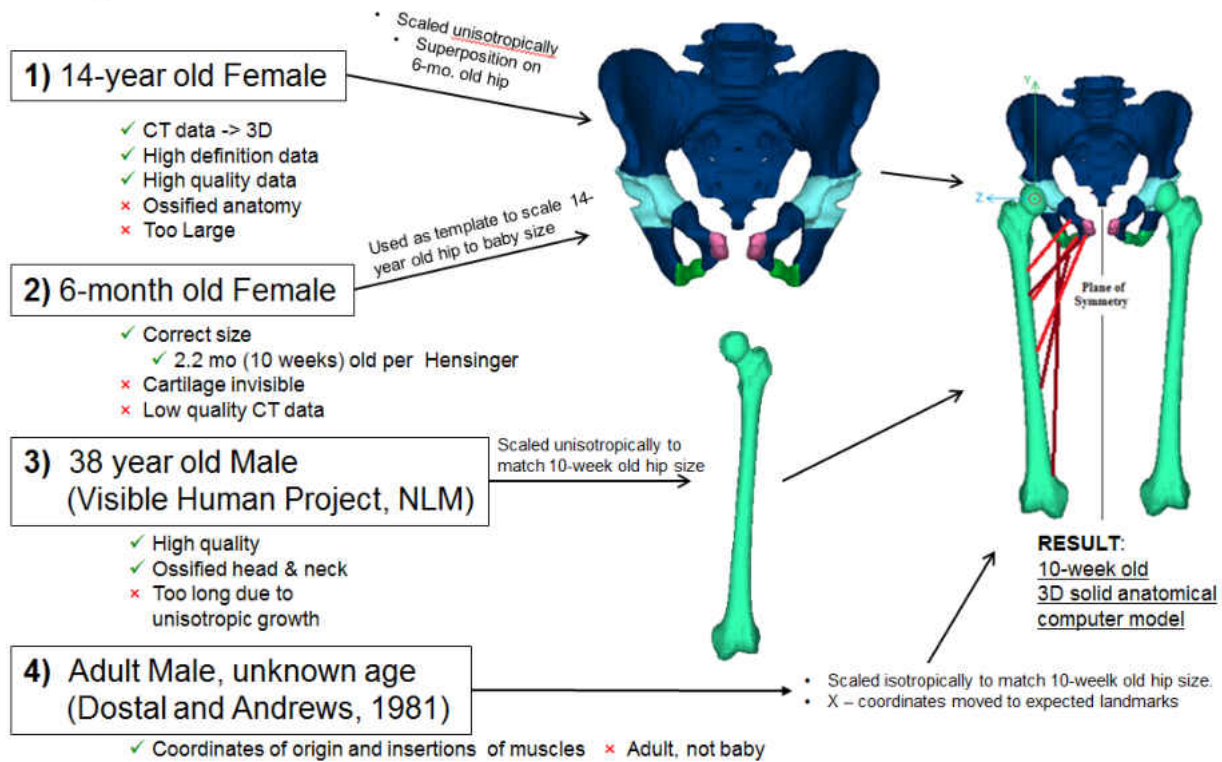
Figure 39 - Development of model of a 10 week-old female infant from data belonging to four human subjects

Locations of origins and insertions of muscles were assigned by scaling adult male data (4) [63] isotropically to match the proportions of the 6-month old infant, using the distances between acetabular centers as scaling parameters. The resulting scaling factor was 0.39. The scaled muscle origin and insertion points matched the expected anatomical landmarks accurately, except in the X-direction at the insertions. In this location some muscles were found to lie slightly off the linea aspera. These muscles were manually adjusted to match the linea aspera,

and this procedure is not expected to cause significant error in the results as the moment variation due to the modified moment arms is not believed to be significant.

This 3-dimensional computer model of the lower anatomy of a 10 week-old female infant is currently being used to carry out four parallel investigations; namely (1) the development of a complete finite element and dynamics computer model for simulations of hip dysplasia reductions using novel treatment approaches, (2) the determination of a path of least resistance in reductions of hip dysplasia based on a minimum potential energy approach, (3) the study of the mechanics of hyperflexion of the hip as alternative treatment for late-presenting cases of hip dysplasia, and (4) a comprehensive investigation of the effects of femoral anteversion angle (AV) variations in reductions of hip dysplasia.

Development of a Complete Finite Element and Dynamics Computer Model for Simulations of
Hip Dysplasia Reductions Using Novel Treatment Approaches

The 3-dimensional finite element and dynamics computer model developed from four human subjects is currently being used to carry out finite element and dynamic simulations of hip dysplasia that further investigate treatment with the Pavlik orthopedic harness, and includes investigation of reductions of hip dysplasia using treatment approaches previously not studied using biomechanics methods.

Determination of a Path of Least Resistance in Reductions of Hip Dysplasia Based on a

Minimum Potential Energy Approach

We are currently using the anatomical geometry around the acetabulum, gravitational potential energy, and strain energy in the muscles, to find a path of minimum potential energy which can be used to vector the femoral head to the acetabulum (Figure 40).
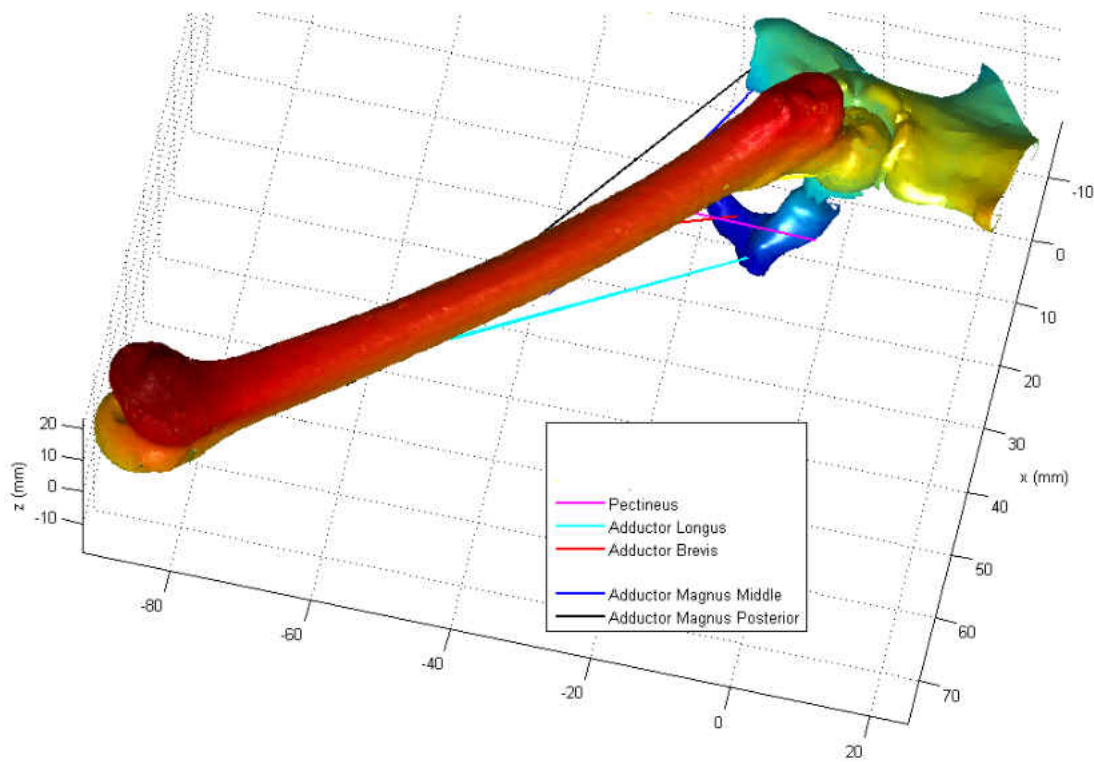
Figure 40 - MATLAB rendering of femur and acetabulum for minimum potential energy

analysis. Color gradient represents depth in Z direction.

Mechanics of Hyperflexion of the Hip as Alternative Treatment for Late-Presenting Cases of Hip

Dysplasia

The 3-dimensional computer model of the lower anatomy of a 10 week-old female infant is currently being employed to investigate the mechanics involved in hyperflexion of the hip. This method is being studied as an alternative method to treat cases of late presenting DDH (Figure 41).
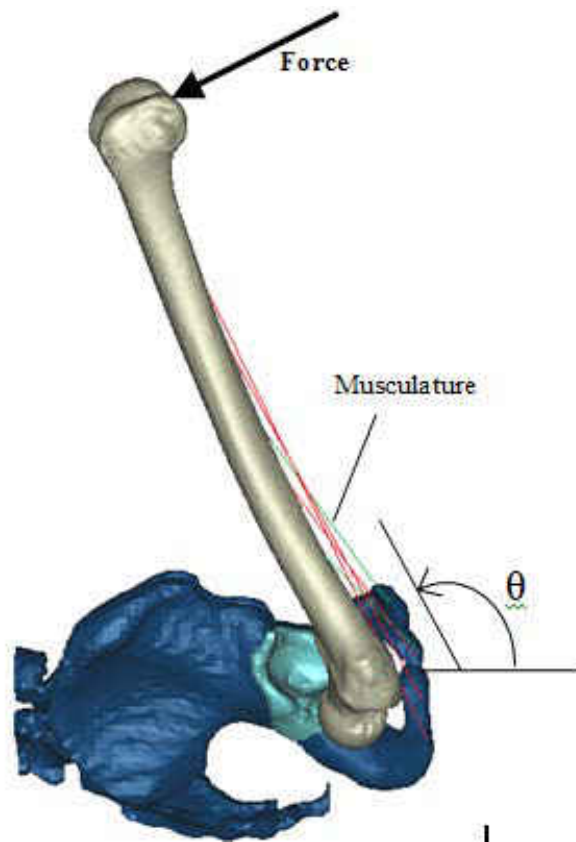
Figure 41 - Development of model to evaluate hyperflexion of the hip as alternative

treatment approach

Comprehensive Investigation of the Effects of Femoral Anteversion Angle (AV) Variations in Reductions of Hip Dysplasia

It is known that femoral anteversion is greater in infants than in adults. It is further known that children born with hip dysplasia have a femoral anteversion angle that is more pronounced than that observed in healthy infants. Recognizing that femoral anteversion variations in infants may have a significant effect in the reductions of hip dysplasia, we embarked in a comprehensive investigation of the effects of anteversion angle (AV) variations in the reductions of hip dysplasia. For this we performed an artificial derotation osteotomies in the 10-week old resultant femur. We thus generated six femora with anteversion angles of 15°, 34°, 45°, 52°, 60°, and 70° (Figure 42). These femora are currently being used to carry out dynamic and finite element simulations of hip reductions of hip dysplasia using various treatment methods. The results will reveal the effects of variations in AV angle in the treatment of hip dysplasia.
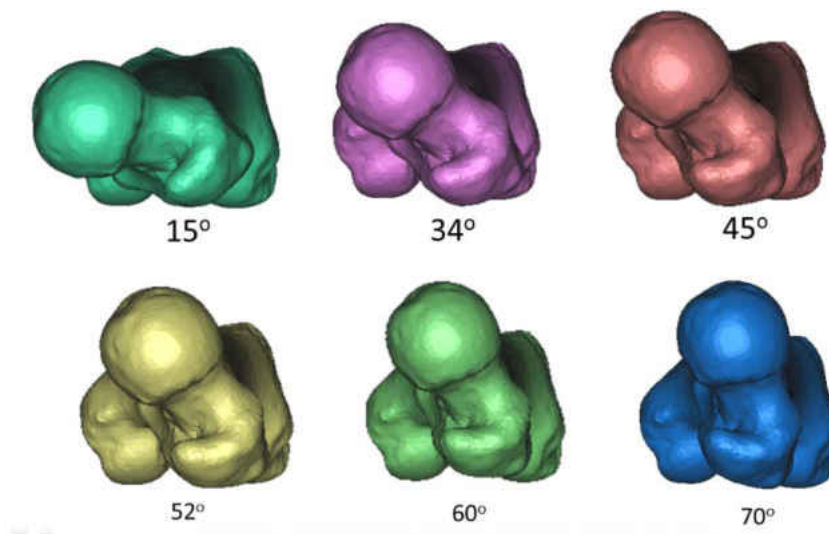
Figure 42 - Femur model with artificial derotation osteotomies to study the effects of AV angle variations in reductions of hip dysplasia

REFERENCES

[1]   Institute, I.H.D. (2010). Beta International Hip Dysplasia Institute.   Retrieved June 1st, 2010, from http://www.hipdysplasia.org/default.aspx

[2]   Weistein, S.L., Mubarak, S.J., & Wenger, D.R. (2003). Developmental Hip Dysplasia and Dislocation Part II. *The Journal of Bone and Joint Surgery, 85*(10), 2024-2035.

[3]   Mubarak, S., Garfin, S., Vance, R., McKinnon, B., & Sutherland, D. (1981). Pitfalls in the Use of the Pavlik Harness for Treatment of Congenital Dysplasia, Subluxation, and Dislocation of the Hip. *The Journal of Bone and Joint Surgery, 64-A*(8), 1239-1248.

[4]   Statistics, N.C.f.H. (2006). Centers for Disease Control and Prevention - Births and Natality (Statistics). FastStats Retrieved June 8th, 2010

[5]   Michaeli, D.A., Murphy, S.B., & Hipp, J.A. (1997). Comnparison of predicted and measured contact pressures in normal and dysplastic hips. *Medical Engineering & Physics, 19*(2), 180-186.

[6]   Clarke, N.M., Harcke, H.T., McHugh, P., Borns, P.F., & MacEwen, G.D. (1985). Real-Time Ultrasound in the diagnosis of congenital dislocation and dysplasia of the Hip. *Journal of Bone and joint Surgery, 67-B*(3), 406-412.

[7]   Crowe, J.F., Mani, V.J., & Snawat, C.S. (1979). Total Hip Replacement in Congenital Dislocation and Dysplasia of the Hip. *The Journal of Bone and Joint Surgery, 61*, 15-23.

[8]   Estes, C., & Tauton, M. (2009). Hip Dysplasia.   Retrieved June 1st, 2010, from http://www.orthopaedia.com/display/Main/Hip+dysplasia

[9]   Ramsey, P., Lasser, S., & MacEwen, G.D. (1976). Congenital Dislocation of the hip. Use of the Pavlik Harness in the Child During the first Six Months of Life. *The Journal of Bone and Joint Surgery, 58*, 1000-1004.

[10]   Rombouts, J., & Kaelin, A. (1992). Interior (Obturator) Dislocation of the hip in Neonates. *Journal of Bone and joint Surgery, 74-B*, 708-710.

[11]   Suzuki, S. (1994). Reduction of CDH by the Pavlik Harness. *The Journal of Bone and Joint Surgery, 76-B*, 460-462.

[12]   Lerman, J.A., Emans, J.B., Millis, M.B., Share, J., Zurakowski, D., & Kasser, J.R. (2001). Early Failure of Pavlik Harness Treatment for Developmental Hip Dysplasia: Clinical and Ultrasound Predictors. *Journal of Pediatric Orthopaedics, 21*, 348-353.

[13]   Hirsch, C., & Evans, F.G. (1965). Studies On Some Physical Properties of Infant Compact Bone. *Acta Orthopaedica Scandinavica, 35*(1-4), 300-313.

[14]   Maquet, P. (1999). Biomechanics of Hip Dysplasia. *Acta Orthopaedica Belgica, 65*(3), 302-314.

[15]   Bombelli, R., Santore, R.F., & Poss, R. (1984). Mechanics of the Normal and Osteoarthritic Hip. *Clinical Orthopaedics and Related Research, 182*, 68-78.

[16]   Fabry, G., MacEwen, G.D., & Shands, A.R. (1973). Torsion of the Femur: A Follow-Up Study in Normal and Abnormal Conditions. *Journal of Bone and joint Surgery, 55*(8), 1726-1738.

[17]   Dunlap, K., Shands, A.R., Hollister, L., Gaul, J.S., & Streit, H.A. (1953). A New Method for Determination of Torsion of the Femur. *Journal of Bone and joint Surgery, 35*(35), 289-311.

[18]   Moulton, A., & S.S., U. (1982). A Direct Method of measuring femoral anteversion using ultrasound. *Journal of Bone and joint Surgery, 64*(4), 469-472.

[19]   Hernandez, R.J., Tachdjian, M.O., Poznanski, A.K., & Dias, L.S. (1981). CT Determination of Femoral Torsion. *American Journal of Roentgenology, 137*(1), 97-101.

[20]   Quesada, P., & Skinner, H.B. (1991). Analysis of a below-knee Patellar tendon-bearing prosthesis: A Finite Element Study. *Journal of Rehabilitation Research, 28*(3), 1-12.

[21]   Brown, T.D., Way, M.E., Fu, F.H., & Jr., A.B.F. (1976). Load Transmission through the Proximal Femur of the Growing Child: A Finite Element Analysis. *Growth, 44*, 301-317.

[22]   Oonishi, H. (1983). Mechanical Analysis of the Human Pelvis and its application to the Artificial Hip Joint - By means of the three dimensional Finite Element Method. *Journal of Biomechanics, 16*(6), 427-444.

[23]   Vaverka, M., Návrat, T., Vrbka, M., Florian, Z., & Fuis, V. (2006). Stress and Strain Analysis of the Hip Joint using FEM. *Technology and Healthcare, 14*, 271-279.

[24]   Almby, B., Hjelmstedt, A., & Lonnerholm, T. (1979). Neonatal hip instability. Reason for failure of early abduction treatment. *Acta Orthop Scand, 50*(3), 315-327.

[25]   Weinstein, S.L. (2006). *Developmental Hip Dysplasia and Dislocation* (6 ed.). Philadelphia: Lippincott Williams and Wilkins.

[26]   Ishii, Y., Weinstein, S.L., & Ponseti, I.V. (1980). Correlation between arthrograms and operative findings in congenital dislocation of the hip. *Clin Orthop Relat Res*(153), 138-145.

[27]   Eberhardt, O., Fernandez, F.F., & Wirth, T. (2012). Arthroscopic reduction of the dislocated hip in infants. *J Bone Joint Surg Br, 94*(6), 842-847.

[28]   Salter, R.B., & Dubos, J.P. (1974). The first fifteen year's personal experience with innominate osteotomy in the treatment of congenital dislocation and subluxation of the hip. *Clin Orthop Relat Res*(98), 72-103.

[29]   Presedo, A., Oh, C.W., Dabney, K.W., & Miller, F. (2005). Soft-tissue releases to treat spastic hip subluxation in children with cerebral palsy. *J Bone Joint Surg Am, 87*(4), 832-841.

[30]   Cobeljic, G., Bajin, Z., Lesic, A., Tomic, S., Bumbasirevic, M., & Atkinson, H.D. (2009). A radiographic and clinical comparison of two soft-tissue procedures for paralytic subluxation of the hip in cerebral palsy. *Int Orthop, 33*(2), 503-508.

[31]   Jacobson, T., & Allen, W.C. (1990). Surgical correction of the snapping iliopsoas tendon. *Am J Sports Med, 18*(5), 470-474.

[32]   Alpert, J.M., Kozanek, M., Li, G., Kelly, B.T., & Asnis, P.D. (2009). Cross-sectional analysis of the iliopsoas tendon and its relationship to the acetabular labrum: an anatomic study. *Am J Sports Med, 37*(8), 1594-1598.

[33]   Dora, C., Houweling, M., Koch, P., & Sierra, R.J. (2007). Iliopsoas impingement after total hip replacement: the results of non-operative management, tenotomy or acetabular revision. *J Bone Joint Surg Br, 89*(8), 1031-1035.

[34]   Rosendahl, K., Markestad T, Lie RT,. (1996). Developmental dysplasia of the hip. A population-based comparison of ultrasound and clinical findings. *Acta Paediatr., 85*, 64-69.

[35]   Bialik, V., Bialik GM, Blazer S, Sujov P, Wiener F, Berant M. (1999). Developmental Dysplasia of the Hip: A New Approach to Incidence. *Pediatrics, 103*, 93-99.

[36]   Boeree, K., Clarke NMP. (1994). Ultrasound imaging and secondary screening for congenital dislocation of the hip. *J. Bone Joint Surg., 76B*, 525-533.

[37]   Patel H. (2001). Prevention health care, 2001 update: screening and management of developmental dysplasia of the hip in newborns. *CMAJ, 164*, 1669-1677.

[38]   Chan, A., Foster BK, Cundy PJ,. (2001). Problems in the diagnosis of neonatal hip instability. *Acta Paediatr., 90*, 836-839.

[39]   Peled, E., Eidelman M, Katzman A, Bialik V,. (2008). Neonatal incidence of hip dysplasia. *Clin. Orthop. Rel. Res., 466*, 771-775.

[40]   Chan A, F.B., Cundy PJ,. (2001). Problems in the diagnosis of neonatal hip instability. *Acta Paediatr., 90*, 836-839.

[41]   Engesaeter IO, L.S., Lehmann TG, Furnes O, Vollset SE, Engesaeter LB,. (2008). Neonatal hip instability and risk of total hip replacement in young adulthood. *Acta. Orthop., 79*, 321-326.

[42]   Wedge JH, W.M. (1978). The natural history of congenital dislocation of the hip. *Clin. Orthop. Rel. Res., 137*, 154-161.

[43]   Ramsey PL, L.S., MacEwen GD,. (1976). Congenital Dislocation of the Hip: use of the Pavlik Harness in the child during the first six months of life. *J. Bone Joint Surg., 58A*, 1000-1004.

[44]   Wilkinson AG, S.D., Murray GD,. (2002). The efficacy of the Pavlik Harness, the Craig splint and the von Rosen splint in the management of neonatal dysplasia of the hip. *J. Bone Joint Surg., 84B*, 716-719.

[45]   Eberle CF. (2003). Plastazote abduction orthosis in the management of neonatal hip instability. *J. Pediatr. Orthop., 23*, 607-616.

[46]   Smith, M. (1981). Use of the Pavlik harness in nonoperative management of congenital dislocation of the hip. *J. Royal Soc. Med., 74*, 591-594.

[47]   Cashman JP, R.J., Taylor G, Clarke NMP,. (2002). The natural history of developmental dysplasia of the hip after early supervised treatment in the Pavlik harness. *J. Bone Joint Surg., 84B*, 418-425.

[48]   Grill F, B.H., Canadell J, Dungl P, Matasovic T, Vizkelety T,. (1988). The Pavlik harness in the treatment of congenital dislocating hip: report on a multicenter study of the European Paediatric Orthopaedic Society. *J. Pediatr. Orthop., 8*, 1-8.

[49]   Peled E, B.V., Katzman A, Eidelman M, Norman D,. (2008). Treatment of Graf's ultrasound class III and IV hips using Pavlik's method. *Clin. Orthop. Rel. Res., 466*(4), 825-829.

[50]   Harding MGB, H.H., Bowen JR, Guille JT, Glutting J,. (1997). Management of dislocated hips with the Pavlik harness treatment and ultrasound monitoring. *J. Pediatr. Orthop., 17*, 189-198.

[51]   Lerman JA, E.J., Millis MB, Syare J, Zurakowski D, Kasser JR,. (2001). Early failure of Pavlik harness treatment of developmental hip dysplasia: clinical and ultrasound predictors. *J. Pediatr. Orthop., 21*, 348-353.

[52]   Atalar H, S.U., Yavuz OY, Uras I, Dogruel H,. (2007). Indicators of successful use of the Pavlik harness in infants with developmental dysplasia of the hip. *Intl. Orthop., 31*, 145-150.

[53]   Viere RG, B.J., Herring JA, Roach JW, Johnston CE,. (1990). Use of the Pavlik harness in congenital dislocation of the hip. *J. Bone Joint Surg., 72A*, 238-244.

[54]   Iwasaki K. (1983). Treatment of congenital dislocation of the hip by the Pavlik Harness. *J. Bone Joint Surg., 65A*, 760-767.

[55]   Weinstein SL. (2006). Developmental Hip Dysplasia and Dislocation. In W. S. Morrissy RT (Ed.), *Pediatric Orthopedics* (Sixth ed., Vol. 2, pp. 987-1037). Philadelphia: Lippincott, Williams & Wilkins.

[56]   Weinstein, S., Mubarak SJ, Wenger DR. (2004). Developmentl hip dysplasia and dislocation: Part I. *Instr. Course Lect., 53*, 523-530.

[57]   Weinstein, S., Mubarak SJ, Wenger DR. (2004). Developmental hip dysplasia and dislocation: Part II. *Instr. Course Lect., 53*, 531-542.

[58]   Osterkamp, L.K. (1995). Current Perspective on Assessment of Human Body Proportions of Relevance to Amputees. *Journal of the American Dietetic Association, 95*(2), 215-218.

[59]   Clauser, C.E., McConville, J.T., & Young, J.W. (1969). Weight, volume, and center of mass of segments of the human body. Wright-Patterson Air Force Base, Ohio: Air Force Systems Command.

[60]   Drillis, R., & Contini, R. (1966). Body Segment Parameters (D. o. H. Office of Vocational Rehabilitation, Education and Welfare, Trans.). New York: New York University School of Engineering and Science.

[61]   Dempster, W.T. (1955). Space requirements of the seated operator (U. S. A. Force, Trans.). Wright-Patterson Air Force Base, Ohio: Wright Air Development Center.

[62]   CDC. (2009). *Birth to 24 months: Girls Length-for-age percentiles and Wight-for-age percentiles*. Centers for Disease Control and Prevention. Retrieved from http://www.cdc.gov/growthcharts/who_charts.htm.

[63]   Dostal, W.F., & Andrews, J.G. (1981). A three-dimensional biomechanical model of hip musculature. *Journal of Biomechanics, 14*(11), 803-812.

[64]   Suzuki, S. (1994). Reduction of CDH by the Pavlik Harness. Spontaneous reduction observed by ultrasound. *The Journal of Bone and Joint Surgery, 76-B*(3), 460-462.

[65]   Iwasaki, K. (1983). Treatment of congenital dislocation of the hip by the Pavlik Harness. Mechanism of reduction and usage. *The Journal of Bone and Joint Surgery, 65A*, 760-767.

[66]   Magid, A., & Law, D.J. (1985). Myofibrils Bear Most of the Resting Tension in Frog Skeletal Muscle. *Science, 230*, 1280-1282.

[67]   Hill, A.V. (1952). The Thermodynamics of Elasticity in Resting Striated Muscle. *Proceedings of the Royal Society of London. Series B, Biological Sciences, 139*, 464-497.

[68]   Sten-Knudsen, O. (1953). Torsional elasticity of the isolated cross striated muscle fibre. *Acta Physiologica Scandinavica, 25*, Supplement 104.

[69]   Hill, A.V. (1949). Is Relaxation an Active Process? *Proceedings of the Royal Society of London. Series B, Biological Sciences, 136*, 420-435.

[70]   MSC Software. (2012). Adams/Solver help - Adams 2012.1.2. DOC10024, 2012

[71]   Marieb, E.N., & Hoehn, K. (2007). Human Anatomy & Physiology *Human Anatomy & Physiology* (7 ed.). San Francisco: Benjamin Cummings.

[72]   Dostal, W.F., & Andrews, J.G. (1981). A three-dimensional biomechanical model of hip musculature. *J Biomech, 14*(11), 803-812.

[73]   Eberhardt, O., Fernandez, F.F., & Wirth, T. (2012). Arthroscopic reduction of the dislocated hip in infants. *The Journal of Bone and Joint Surgery, 94-B*(6), 842-847.

[74]   Papadimitriou, N.G., Papadimitriou, A., Christophorides, J.E., Beslikas, T.A., & Panagopoulos, P.K. (2007). Late-Presenting Developmental Dysplasia of the Hip Treated with the Modified Hoffmann-Daimler Functional Method. *Journal of Bone and joint Surgery, 89*, 1258-1268.

[75]   Gruen, G.S., Scioscia, T.N., & Lowenstein, J.E. (2002). The surgical treatment of internal snapping hip. *Am J Sports Med, 30*(4), 607-613.

[76]   Wahl, C.J., Warren, R.F., Adler, R.S., Hannafin, J.A., & Hansen, B. (2004). Internal coxa saltans (snapping hip) as a result of overtraining: a report of 3 cases in professional

athletes with a review of causes and the role of ultrasound in early diagnosis and management. *Am J Sports Med, 32*(5), 1302-1309.

[77]   McCarthy, J., Noble, P., Aluisio, F.V., Schuck, M., Wright, J., & Lee, J.A. (2003). Anatomy, pathologic features, and treatment of acetabular labral tears. *Clin Orthop Relat Res*(406), 38-47.

[78]   Forlin, E., Choi, I.H., Guille, J.T., Bowen, J.R., & Glutting, J. (1992). Prognostic factors in congenital dislocation of the hip treated with closed reduction. The importance of arthrographic evaluation. *J Bone Joint Surg Am, 74*(8), 1140-1152.

[79]   Liu, J.S., Kuo, K.N., & Lubicky, J.P. (1996). Arthrographic evaluation of developmental dysplasia of the hip. Outcome prediction. *Clin Orthop Relat Res*(326), 229-237.

[80]   Treguier, C., Baud, C., Ferry, M., Ferran, J.L., Darnault, P., Chapuis, M., . . . Violas, P. (2011). Irreducible developmental dysplasia of the hip due to acetabular roof cartilage hypertrophy. Diagnostic sonography in 15 hips. *Orthop Traumatol Surg Res, 97*(6), 629-633.

[81]   Salter, R.B. (1966). Role of innominate osteotomy in the treatment of congenital dislocation and subluxation of the hip in the older child. *J Bone Joint Surg Am, 48*(7), 1413-1439.

[82]   Bassett, G.S., Engsberg, J.R., McAlister, W.H., Gordon, J.E., & Schoenecker, P.L. (1999). Fate of the psoas muscle after open reduction for developmental dislocation of the hip (DDH). *J Pediatr Orthop, 19*(4), 425-432.

[83]   Hensinger, R.N. (1986). *Standards in Pediatric Orthopedics*. New York: Raven Press.